DISEERTATION FOR THE DOCTORAL DEGREE

Study on Functional Roles of MicroRNA-342 via Targeting Chemokine CXCL12 in Tumorigenesis

NAME: TIAN YIJUN

DOCTROAL PROGRAM IN LIFE AND FOOD SCIENCE

GRADUATE SCHOOL OF SCIENCE AND TECHNOLOGY

NIIGATA UNIVERSITY

Contents

Abbreviation

Abbr.	FULL NAME	Abbr.	FULL NAME
MiR-342	MicroRNA-342	PI	Propidium iodide
Evl	Ena-vasodilator stimulated phosphoprotein	DAB	3,3’-Diaminobenzidine
CXCL12	Chemokine (C-X-C motif) ligand 12	DAPI	4',6-diamidino-2-phenylindole
SDF-1	Stromal cell-derived factor 1	CD31	Cluster of differentiation 31
CXCR4	Chemokine (C-X-C motif) receptor 4	3’UTRs	3’-untranslated regions
CXCR7	Chemokine (C-X-C motif) receptor 7	DLR	Dual-luciferase reporter assay
VEGF	Vascular endothelial growth factor	TGF-β	Transforming growth factor-beta
CD11b	Integrin alpha M	FGF	Fibroblast growth factor
ANG	Angiopoietins	EGF	Epidermal growth factor
CD80	Cluster of differentiation 80	CD86	Cluster of differentiation 86
CD163	Cluster of differentiation 163; scavenger receptor	FIZZ1	Found in inflammatory zone 1
Mφ	Macrophages	YM1/Chi3l3	Chitinase 3 - like 3
BSA	Bovine serum albumin	Thbs-1	Thrombospondin 1
IL-18	Interleukin-18	CCL-11	C-C chemokine ligand 11
TAMs	Tumor-associated macrophages	H&E	Hematoxylin and Eosin
α-MEM	Alpha Modified-Minimum Essential Medium	DMEM	Dulbecco's Modified Eagle's Medium

Abstract

A neoplasm or tumor is a group of cells that have undergone unregulated growth and frequently form a mass or lump. The past decades, numerous molecular biology mechanisms have been uncovered to seek an understanding in tumor, such as, growth pathways, cell cycle, cell apoptosis, angiogenesis, cancer stem cells and more recently exosome-mediated molecules' transportation, and targeted immunotherapy. However, much work remains to do toward understanding the mechanistic underpinnings of each hallmarks.

MicroRNAs (miRNAs), a classical ~22 nucleotides noncoding RNAs, are post-transcriptional regulators of protein-coding gene expression. The regulatory role of miRNAs makes it an important player in tumor development process: initiation, development, progression and metastasis.

The sarcoma cell lines, MS-K and LM-8, are two commonly used models in search of gene candidates involved in tumorigenesis or angiogenesis in C3H mice. Tumors formed by MS-K cells grow faster, and showed more enriched blood vessels in contrast to LM-8 tumors. While, miRNAs expression analysis indicated that the MS-K expressed a lower level of miR-342 compared to that in the LM-8. The miR-342 has been reported as a tumor-suppressor or an oncogenesis related-miRNA based on functions or expression changes in multiple types of cancers,

Here, I provide evidence that miR-342 serves as a tumor suppressor via targeting chemokine CXCL12 (also known as Stroma Derived Factor-1alpha; SDF-1α). Stable overexpression of miR-342 in MS-K cells inhibited cell proliferation, and capacity of colony formation *in vitro*. Moreover, induced miR-342 promoted cell cycle arrest in the G0/G1 phase and cell apoptosis. Bioinformatics analysis indicated chemokine CXCL12 mRNA was a putative target of miR-342. RT-PCR and western blotting analysis revealed a reversely correlation between endogenous CXCL12 expression and mature miR-342

RNA levels in MS-K and/or LM-8. Dual-luciferase reporter assay experiments validated the interaction between miR-342 and CXCL12 3'-UTR.

The chemokine CXCL12 is a well studied α-chemokine that binds to receptors CXCR4/7, and has been implicated in the recruitment of monocytes / macrophages and tumorigenesis. *In vivo* experiments, overexpression of miR-342 significantly suppressed MS-K tumor growth. More importantly, more CD11b-positive macrophages was accumulated in tumors formed by MS-K-miR-342 cells, either in total number of CD11b-positive cells or proportion against total tumor cells, compared to controls. Furthermore, the expression of proangiogenic genes (*Vegf-A* and *Thbs1*) and M2-subtype macrophage markers (*Cd163, Dectin1* and *Ym1*) was significantly decreased in the CD11b-positive cells derived from MS-K-miR-342 tumors compared to controls. In addition, down-regulated level of *Cxcl12* and its receptor *Cxcr4* was also observed, but the miR-342 level was not markedly affected in the CD11b-positve cells from MS-K-miR-342 tumors in contrast to controls. These results implying that the miR-342 derived from MS-K-miR-342 cells but not endogenous miR-342, might be contribute to *Cxcl12* suppression in tumor-infiltrated macrophages. Finally, restored CXCL12 expression in MS-K-miR-342 cells rescued cell proliferation, and cell cycle arrest *in vitro*.

Together, these studies demonstrate that miR-342 is involved in MS-K tumor growth as a tumor-suppressor by targeting chemokine CXCL12.

1. Introduction

1.1 Discovery, biogenesis and action mechanism of microRNAs

MiRNAs are endogenous ~22 nucleotides noncoding RNA molecules that can play important regulatory roles in animals and plants by targeting mRNAs of protein-coding genes for cleavage or translational repression [1, 2]. In mammals, over 1,000 miRNAs have been identified [3].

MicroRNAs are transcribed for the most part by RNA polymerase II as long primary transcripts characterized by hairpin structures (pri-miRNAs), and processed into the nucleus by RNase III Drosha into 70-100 nucleotides (nts) long pre-miRNAs [4].

The originated precursor molecules are exported by an Exportin 5-mediated mechanism to the cytoplasm [5], where an additional step mediated by the RNase III Dicer, which acts in complex with the transactivating response RNA‐binding protein (TRBP), generates a dsRNA approximately 22 nts long, named miRNA/miRNA*, including the mature miRNA guide, and the complementary passenger strand, the miRNA* (star miRNA). Whereas one of the two strands is selected as guide strand according to thermodynamic properties, the complementary one is usually subjected to degradation. The so-called miRNA* was initially thought to be the strand subjected to degradation, instead more recent evidence suggests that it does not simply represent a non-functional bio-product of miRNA biogenesis, but it can be selected as a functional strand and play significant biological roles [6].

Completed the processing steps, the mature single stranded miRNA product is then incorporated in the complex known as miRNA-containing ribonucleoprotein complex (miRNP), miRNA-containing RNA-induced silencing complex (miR-RISC), a ribonucleoprotein complex containing Argonaute proteins, of which AGO1 and 2 have been the most extensively studied, the two

miRNA strands and several additional factors, including the trans‐activator RNA binding protein (TRBP) [7-10].

Moreover, even though it is known that microRNAs mainly recognize complementary sequences in the 3'-untranslated regions (UTRs) of their target mRNAs, more recent studies have reported that they can also bind to the 5'-UTR or the ORF [11], resulting in translation repression or target degradation [7, 12].

Considering the different rules regulating the interaction between a microRNA and its target mRNA, it is not surprising that each miRNA has the potential to target a large number of genes. Equally, roughly 60% of the mRNAs share one or more sequences that are evolutionarily conserved and predicted to interact with miRNAs. Bioinformatics analysis predicts that 3'-UTRs of single genes are often targeted by several different miRNAs [13, 14]. Many of these predictions have been validated experimentally, suggesting that miRNAs might cooperate to regulate gene expression.

1.2 Roles of microRNAs in tumors

Early studies have demonstrated that aberrantly expressed microRNAs are a hallmark of several diseases, such as cancer. MicroRNA expression profiling was associated with tumor development, progression and response to therapy, suggesting their possible use as diagnostic, prognostic and predictive biomarkers [15]. Dysregulated miRNAs may function as either tumor suppressors or oncogenes in cancer by targeting each one of these features. Moreover, the increasing number of studies demonstrating that miRNA-based anticancer therapies have recently been exploited, either alone or in combination with current targeted therapies.

1.2.1 MicroRNAs as tumor suppressor genes

In chronic lymphocytic leukemia (CLL), the chromosome 13q14 locus was found frequently deleted. miR-15a and miR-16-a located in this critical region were firstly proved deletion miRNA in human cancer [16]. Recent studies showed that miR-15a and miR-16-a were frequently knocked down or knocked out lost in prostate cancer and many melanomas [15, 16].

Gain- and loss-of-function experiments, together with target prediction analyses, have provided insights into the role of miRNAs in carcinogenesis. Gain-of-function approaches have shown that miRNAs acting as tumor suppressors target oncoproteins with crucial roles in various cancer pathways. For instance, miR-15a and miR-16-1 could target oncoprotein BCL2 in lymphocyte to induce apoptosis in human leukemia [17]. The let-7 family was frequently lower expressed in lung tumors and negatively regulated RAS protein, providing a possible mechanism for let-7 in cancer [18]. Furthermore, the miR-29 family, containing miR-29a, miR-29b and miR-29c, was often found deleted in most of hematopoietic solid tumors, and inhibited cell apoptosis through suppressing apoptotic gene, myeloid cell leukemia sequence 1 (Bcl2-related, MCL-1) [19, 20]. In addition, the MYC oncogene was down-regulated in Namalwa cells, a Burkitt lymphoma. Let-7a was elected using bioinformatics for targeting MYC, and induced let-7a led to down-regulation of expression of MYC and its target genes and anti-proliferation in lymphoma cells [21]. This supports previous results in lung and colon cancer where decreased levels of the let-7 family resulted in increased tumorigenicity [15].

1.2.2 MicroRNAs as oncogenes

MicroRNAs with oncogenic function are termed as oncogenic miRNAs. Oncogenic miRNAs were frequently overexpressed in cancer cells. To assess the biological effects of oncogenic miRNAs *in vitro* silencing was a primary approach and carried out using antisense oligonucleotides. For instance, miR-

21 expression has been reported at high levels in breast cancer [22], glioblastomas [23], pancreas [24] and colon cancer [25] among others. Additional studies showed that miR-21 anti-apoptotic effects occurs by targeting the tumor suppressors phosphatase and tensin homologue (PTEN) and programmed cell death 4 (PDCD4) [26, 27]. More recently, Slack's group [28] has shown that mice conditionally expressing miR-21 develop a pre-B malignant lymphoid-like phenotype, thus demonstrating that miR-21 is a genuine oncogene.

MiR-17-92 cluster and miR-155 were the first examples of miRNAs with oncogenic activity validated in engineered animal models [29, 30]. Moreover, both of them were discovered to be overexpressed in lymphoproliferative disorders, including lymphomas and leukemia [30]. Transgenic mice overexpressing miR-17-92 cluster in B cells were discovered to develop lymphoproliferative disease and autoimmunity [31]. Mu and colleagues showed that deletion of the complete miR-17-92 cluster slows down Myc-induced oncogenesis [32].

Taken together, increasing studies indicated that there was a correlation between miRNAs expression and tumorigenesis. It is unlikely that miRNAs will be found responsible for a specific phenotype by aiming at a specific target. Instead, it is largely accepted that miRNAs engage in complex interactions with the machinery that controls the transcriptome and concurrently target multiple mRNAs. This is probably the most intriguing rationale supporting the idea of using microRNAs as anticancer drugs.

1.3 Macrophages and tumorigenesis.

Over time, cancers have developed sophisticated networks of biological activities allowing their growing and evading from drug treatment. This complex program relies on the communication between multiple cell types, including the primary tumor as well as the stromal cells. Macrophages are the major

infiltrating immune cells known as tumor-associated macrophages (TAMs), and they play important roles in the tumor microenvironment [33, 34]. Macrophages can exert both anti- and pro-tumoral functions according to their distinct polarized subtypes: the classically activated (M1) macrophages and alternatively activated (M2) macrophages [35]. M1 macrophages induce inflammatory activation and kill pathogens. In contrast, M2 macrophages suppress inflammatory activation and promote angiogenesis [36]. TAMs are involved in tumor angiogenesis through the production of various proangiogenic growth factors: VEGF-A, VEGF-C, EGF(Epidermal growth factor), TGF-β(Transforming growth factor-beta), PFGF(Platelet-derived growth factor) and angiogenic chemokines [37-39]. M2 macrophages show high expression of YM1, FIZZ1, Dectin-1 and scavenger receptors [35, 40] as well as express the hemoglobin scavenger receptor CD163 [41, 42]. In the tumor microenvironment, macrophages are educated by the cytokine/chemokine milieu where TAMs have been shown generally to acquire the hallmarks of alternatively activated M2 macrophages. For instance, certain cytokines, IL-4 and IL-3, are strong inducers of an alternative (M2) form of macrophage activation [39]. A series of chemokines orchestrate the recruitment of monocytes/macrophages and the chemokine CCL2 (also known as MCP-1) was first discovered as a tumor-derived chemotactic factor which recruits these cells to tumor tissues [39]. Stromal cell-derived factor-1 (SDF-1), also known as CXCL12, drives TAM accumulation and survival in hypoxic areas of tumors [43].

The chemokine CXCL12 is an important α-chemokine that binds to its receptors CXCR4 and CXCR7 [44]. It has been reported that miR-137, miR-448 and miR-101 could directly target CXCL12 in many kinds of cancers, including papillary thyroid carcinoma, ovarian cancer and lung cancer [45-47]. CXCL12 treatment of IGROV cancer cells induced *in vitro* growth, which was attributable to stimulation of DNA synthesis [48]. Moreover, the introduction of miR-454 dramatically suppressed the migration of CXCR4+ macrophages and the ability of pancreatic ductal adenocarcinoma (PDAC) cells to form tumors via

downregulating SDF-1 [49].

1.4 Overview of this research.

MiR-342 is located on the imprinted mouse distal 12 domain and is considered an imprinted gene candidate [50]. Aberrant expression of miR-342 has been found in multiple cancers, and down-regulated or epigenetically silenced miR-342 expression induces some key oncogenic proteins [51-55]. However, evidence of miR-342 participating in macrophage-mediated regulation of tumorigenesis remains limited.

In the present study, miR-342 was screened as a tumor-regulatory candidate by comparison two murine sarcoma tumors: MS-K and LM-8, where showed difference in tumor weight and blood vessel development. Next, MS-K-miR-342 cell clones were established to investigate the role of miR-342 in tumorigenesis and angiogenesis. Overexpression of miR-342 in MS-K inhibited cell proliferation *in vitro* and suppressed tumor growth *in vivo*. Moreover, enhanced miR-342 impeded blood vessels formation and accumulation of macrophages in tumors. By bioinformatic analysis and dual-luciferase reporter assays, chemokine CXCL12 was identified as a direct target of miR-342. Restored *Cxcl12* expression in MS-K-miR-342 cells rescued cell proliferation. The expression of proangiogenic genes (*Vegf-A* and *Thbs1*) and M2-subtype macrophage markers (*Cd163, Dectin1* and *Ym1*) was significantly downregulated in the tumor-infiltrated macrophages derived from MS-K-miR-342 tumors. These results suggest that miR-342 is a tumor suppressor by targeting chemokine CXCL12 involved in macrophages accumulation and activation.

2. Materials and Methods

2.1 Mice

The C3H/HeN mice were purchased from SLC (SLC Co. Ltd, Sizuoka, Japan) and fed under pathogen-free condition. 8- to 12-week-old mice were used *in vivo* experiments. All animal experiments were approved by Ethics Committee of Niigata University.

2.2 Cell cultures

The parental MS-K, stable miR-342-overexpressing MS-K cell clones (MS-K-miR-342) and control clones (MS-K-mock) were cultured in alpha-modified minimal essential medium (α-MEM) supplemented with 10% horse serum (HS), 100 units/mL penicillin, and 100 units/mL streptomycin. LM-8 cells were maintained in MEM supplemented with 10% FBS, 100 units/mL penicillin, 100 units/mL streptomycin. All of the cell lines were incubated at 37˚C with 5% CO2.

2.3 Total RNA extraction and cDNA synthesis

For mRNA expression analysis, total RNAs were isolated from MS-K, LM-8 cell lines, and tumor-derived CD11b+ cells using TRIzol reagent (Invitrogen, Carlsbad, CA). The cDNA samples were synthesized using a TOYOBO cDNA kit (TOYOBO, Osaka, Japan). The expression of related genes in MS-K cells, LM-8 cells, or MS-K-mock, MS-K-miR-342 clones was analyzed by RT-PCR with gene-specific PCR primers. Gene expression in the tumor-derived CD11b+ cells was determined by quantitative real-time PCR (qPCR). Then the relative expression of the genes against *β–actin* was calculated.

For miRNAs expression analysis, total RNAs were isolated from established MS-K-mock and MS-K-miR-342 cell clones using Trizol reagent and a Mir-X miRNA First-Strand Synthesis Kit (Clontech, Mountain View, CA). Moreover, preparation of total

RNAs of tumor tissues was described in previous paper [56].The expression of miR-342 was analyzed by using a LightCycler (Roche Diagnostics GmbH, Manheim, Germany). Expression of snoRNA202 was used as a loading control. All of primers used for RT-PCR or qRT-PCR are listed in supplemental material Table S1.

2.4 Construction of pmR-ZsGreen1-miR-342 and pIRES2-EF-1α-Kusabira Orange-CXCL12

To stable overexpress miR-342 in MS-K cells, pmR-ZsGreen1 vector (Clontech Inc., CA, USA) was used. The fragment contained pre-miR-342 were amplified from genomic DNA of mouse bone marrow cells using primer For: CCC AAG CTT GCC TTC CAT ATC TGT ATT T; Rev: CCG GGA TCC TCT CAC TCT GCT GGT CAT. Then the PCR products were cloned into BamH I / Hind III site of pmR-ZsGreen1 vector, termed as pmR-ZsGreen1-miR-342. The inserted DNA sequences were verified by DNA sequencing. The mock vector contains no transgene in the expression cassette.

To rescue CXCL12 expression in MS-K-miR-342 cells, pIRES2-EF-1α-Kurobisa Orange vector was used. The mature CXCL12 DNA fragment was amplified by PCR with following primer using PrimeSTAR HS DNA Polymerase (Takara, Japan): Forward primer: CGT CAG ATC CGC TAG CGC CAC CAT GAA ACC AGT CAG C, Reverse primer: GGA GAG GGG CGG ATC CTT ACT TGT TTA AAG CTT TC. The targeted PCR products were purified from 2% agarose gel by Wizard SV Gel and PCR Clean-Up System (Promega, USA) according to the manufacturer's instructions. Then, PCR products were ligated into pIRES2-EF-1α-Kusabira-Orange vector to generate pIRES2-EF-1α-KO-CXCL12 by In-Fusion method using NEBuilder HiFi DNA Assembly Master (New England Biolabs). The sequence of inserted DNA fragment was validated by DNA sequencing. The construct pIRES2-EF-1α-KO-CXCL12 is ready for cell transfection.

2.5 Establishment of MS-K-miR-342 and MS-K-miR-342-CXCL12 clones

MS-K-miR-342 cell lines: To obtain MS-K cell lines that stable expressing miR-342, MS-K cells were transfected with pmR-ZsGreen1-miR-342 or empty vector, followed by a geneticin selection (400 μg/mL) for about two weeks. The survived cells were subsequently sorted into 96-well plates at single cell per well by a FACS Aria II system (BD, Tokyo, Japan) by fluorescence protein ZsGreen1 expression to generate MS-K-miR-342 or MS-K-mock cell clones. Then the three miR-342-overexpressing MS-K clones (MS-K-miR-342) and three control cell clones (MS-K-mock) were established. The relative expression of miR-342 was confirmed in these cell clones by qPCR.

MS-K-miR-342-CXCL12 cell lines: To rescue CXCL12 expression in MS-K-miR-342 cells, MS-K-miR-342 cl.4 cells were transfected with pIRES2-EF-1α-KO-CXCL12 vector. The cells, which expressed the ZsGreen1 fluorescent protein and Kusabira Orange (KO) protein, were sorted by FACSAria II (BD, Tokyo, Japan) to make single cell clones. Several cell clones were chosen to check CXCL12 expression by quantitative PCR (qPCR). Final, the four miR-342-CXCL12-overexressing MS-K clones (MS-K-miR-342-CXCL12) were established.

2.6 Growth curve assay

The cell clones of MS-K-miR-342, MS-K-miR-342-CXCL12 and MS-K-mock or parental MS-K were plated in 35 mm dishes at a density of 1 x 10^4 cells per dish (n=3~4). The number of living cells was counted with a hemocytometer by Trypan blue dye exclusion test after 2, 3, 4, and 5 days.

2.7 Colony formation assay

The MS-K-miR-342 clones and MS-K-mock clones were seeded in 35 mm dishes (n = 3) at 1 x 10^3 cells/dish in culture medium containing 0.8%

methylcellulose. The cells were incubated at 37°C, 5% CO_2 in an incubator for 17 days. Then the number of cell colonies with diameter ≥ 100 μm was counted and calculated on day 17.

2.8 Western blotting

Parental MS-K, MS-K-mock (cl.1, cl.3) or MS-K-miR-342 (cl.1, cl.4) cells were harvested and lysed. A total of 30 μg of whole protein was subjected to run a 15% SDS-PAGE, and then transferred onto polyvinylidene difluoride (PVDF) membranes. The membrane was blocked with 5% nonfat milk and incubated with primary antibodies at 4°C overnight: 1/2000 rabbit anti-CXCL12 (Abcam, Cambridge, UK), 1/50000 rabbit anti-α-Tubulin (Cell Signaling Technology, Beverly, MA), followed by anti-rabbit IgG-HRP antibody incubation. The protein bands were detected with EzWestLumi plus solution according to the manufacturer's instructions (Cat. no. WSE-7120, ATTO Corporation).

2.9 Cell cycle analysis

The cell clones (MS-K, MS-K-mock cl.3, MS-K-miR-342 cl.4 and MS-K-miR-342/Cxcl12 cl.2) were seeded in 60 mm dishes (n = 3 per cell clone). The cells were collected when cell confluent reached 70~80%, washed with ice-cold PBS and fixed in 70% ethanol (v/v) at 4°C overnight. The fixed cells were washed, resuspended in Propidium Iodide (PI) solution (0.1% (v/v) Triton X-100, 10 μg/ml PI, 100 μg/ml DNase-free RNase A) and incubated at room temperature for 1 hour at the dark. Then the cells were analyzed by flow cytometry (FACSAria II, BD Bioscience).

2.10 Cell apoptosis assay

Cell apoptosis assay was performed according to the protocol previously described [57]. Parental MS-K, MS-K-mock cl.3, MS-K-miR-342 cl.4 cells were harvested from 90 mm dishes, washed twice with chilled PBS and made into

single-cell suspensions by a pipette (P1000). The cell number was counted using trypan blue solution by a hemocytometry. Then, the cells were suspended in Annexin V binding buffer (BioLegend, CA, USA) at a concentration of 2 x 10^6 cells/ml. Then, 100 µL of cells suspension was transferred into a 1.5-ml centrifuge tube, and treated with 5 µL of PE-Annexin V (BioLegend, CA, USA), 5 µL of PI staining solution. The cells were incubated for 20 min at room temperature, protect from light. Then, the cell samples were re-suspended with another 300 µL of binding buffer. Finally, analysis of the ratios of PE- and PI-positive cells were carried out by using a FACSAria II (BD Bioscience, Tokyo, Japan).

2.11 Tumor formation assay *in vivo*

1x 10^6 of the tumor cells (parental MS-K, parental LM-8, MS-K-miR-342 clones and MS-K-mock clones or MS-K-miR-342-CXCL12 clones) were implanted into the left and right flanks of C3H/HeN mice by subcutaneous injection (n=3-4). The tumors were allowed to grow for 22 days. At the time point, the mice were sacrificed. Then, formed tumors were excised, photographed and weighed. Then tumor tissue samples were ready for total RNA extraction, immune cells infiltration analysis by flow cytometry or embedded by paraffin.

2.12 Immunohistochemical staining of paraffin embedded tumor sections

For analysis of blood vessels formation in tumors, immunohistochemical staining (IHC) with anti-CD31 antibody was performed following the protocol described previously [58]. The paraffin tumor sections (4 µm) were sliced, deparaffinized, rehydrated and boiled in 100 mM Tris-HCl (pH 10.0) for 15 min. Anti-CD31 antibody (AnaSpec, Inc., CA, USA) was used as primary antibody (first antibody) according to the manufacturer's instructions. For labelling primary antibody, the peroxidase-conjugated secondary antibody (KPL, MD, USA) and the DAB solution (VECTOR laboratories, CA, USA) were applied.

Then, hematoxylin was used for counterstaining of the nuclear. Microvessel density was quantified by counting the number of CD31 positive staining structures in five random fields in the tumor sections. Appropriate blanks and controls were included in the experiment.

2.13 Analysis and isolation of CD11b-positive cells in the tumors

For analysis and isolation of CD11b+ cells from tumors, flow cytometry was employed according the protocol previously reported [57, 59, 60]. The tumor tissues were prepared into single-cell suspension by mechanically cutting and collagenase (Yakuruto, Tokyo, Japan) treatment. In detail, the tumors were excised from the C3H/HeN mice on day 22 after inoculation. The tumors (700 mg/sample) were mechanically cutting into small pieces in 0.5 ml of cold HBSS. The collagenase (250 U/ml) solution was directly added to the cell suspension and incubated in at 37°C in a water bath for 30-45 min with gently shaking. Then the cell suspension was filtrated with the metal mesh to remove big tumor blocks. The cells were washed twice with the FACS buffer (2% FBS/PBS) and filtrated with nylon mesh (# 200 mesh, J-Medical, Niigata, Japan). The cell number counted using Turk's solution. Designated number of cells was dispensed into centrifuge tubes and centrifuged. After removed supernatant, 2 ml of 2.4G conditioned medium was added into the cells and incubated on ice for 10 min to block non-specific binding of the antibody to Fc receptor. Then cells were washed twice by FACS buffer (2% FBS/PBS) and dispensed into 1.5 ml centrifuge tubes. #1: negative control, non-staining; #2: only stained by Propidium iodide (PI); #3: the allophycocyanin (APC)-conjugated anti-mouse CD11b (1 μL/10^6 cells, 1/200 diluted by FACS buffer, BioLgend, CA, USA); #4: the APC-anti-mouse CD11b and PI staining. The cells were incubated with antibody solution without PI staining at 4°C for 30 min, protect from light. Then, the cells were washed twice with FACS buffer (2% FBS/PBS), and then, re-suspened by appropriate volume of FACS buffer, and treated with PI staining.

Final, the cells were passed through the filter. Flow cytometry analysis and CD11b+ cells sorting were performed by using a FACSAria II (BD, Tokyo, Japan).

2.14 Dual-luciferase reporter assay

For determining CXCL12 is a direct target of miR-342, dual-luciferase reporter assay was carried out as previously described [56]. Two of 3'UTR regions of CXCL12 gene (~300 base pairs of length) containing the predicted *miR-342* binding sites (407-413 and 1159-1165 3'UTR regions) were amplified by using following primers:

Forward primer #1: GGA CTA GTC GGA AGG AAG ATC GGT GGC; Reverse primer #1: CCC AAG CTT CCC TTC CCT AAC ACT GAC, and Forward primer #2: GGA CTA GTG CAT CTA TGT CTT GTT TGG; Reverse primer #2: CCC AAG CTT CAC CTT TCT TTG GGC TTT GT. The wide type of 3'UTR regions were termed as CXCL12-3'-UTR-wt #1, #2 respectively. Mutated-type 3'-UTRs were synthesized and termed as CXCL12-3'-UTR-mut #1, #2 (Integrated DNA Technologies, Japan). 3'-UTRs were cloned between Spe I and Hind III restriction sites into the pMIR-REPORT luciferase vector (Ambion, Austin, TX), to generate pMIR-CXCL12-3'-UTRs-wt or pMIR-CXCL12-3'-UTRs-mut vector. MS-K-miR-342 cl.4 or MS-K-mock cl.3 cells were seeded into 24-well plates and co-transfected with 0.5 μg of the pMIR-CXCL12-3'-UTRs or empty vector and 0.05 μg of pRL-TK Renilla vector using ViaFect Transfection Reagent (Promega, USA). 48 hours later, luciferase activity was measured using the dual luciferase reporter assay system (Promega, Madison, WI) with a GloMax 20/20 luminometer (Promega, USA). The pRL-TK Renilla vector was kindly gifted from Prof. Wu (Harbin University, Chaina).

2.15 Statistical analysis

All results are presented as the mean ± SD. For the paired statistical analysis, student's *t*-test was applied. In all figures, * represents $P < 0.05$, ** $P < 0.01$ and *** $P < 0.001$.

3. Results

3.1 The MS-K and LM-8 on tumor formation and angiogenesis *in vivo*.

Two sarcoma cell lines, MS-K and LM-8, both of them derived from C3H/HeN mouse, are advantageous platforms for carrying out researches on tumorigenesis and angiogenesis *in vitro* and *in vivo*.

To evaluate and comparison of tumor growth and blood vessel development, $1x10^6$ of MS-K and LM-8 cells were injected into fat-pad flanks C3H mice by subcutaneous inoculation. The tumors were allowed to grow over 22 days. At the endpoint, the mice were sacrificed. Tumors were excised and weighed. The representative photos of MS-K and LM-8 tumors were shown (**Figure 2, Left**). By the photos of the tumors, the blood vessels were enriched in the parental MS-K cells formed tumors; in contrast, in the parental LM-8 cells formed tumors, the blood vessels were barely seen.

Tumor tissues weight was statistical calculated (**Figure 2, Right**). The results show that the weight of parental MS-K tumors was significantly higher than that of parental LM-8 tumors.

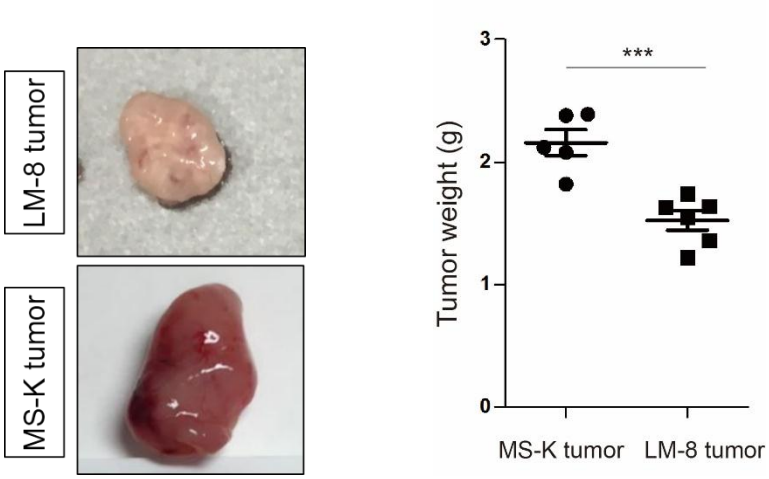

Figure 2. The tumor growth of MS-K and LM-8 cells *in vivo*.

Left: The photos of MS-K tumor and LM-8 tumors excised from C3H/HeN mice on day 22. Right: The weight of MS-K and LM-8 tumors was weighed and statistical analyzed. Data indicated mean ±standard deviation (n = 4-6). *** indicates $p < 0.001$.

An Immunohistochemical staining demonstrated that there was enriched vessel formation in the parental MS-K tumors contrary to poor developed blood vessels in the parental LM-8 tumors (**Figure 3a**). To quantify blood vessel density, the number of CD31 positive staining structures in parental MS-K and LM-8 tumor sections (4 μm) were calculated (**Figure 3b**). The result showed that the microvessel density in parental MS-K tumors was significantly more than that in parental LM-8 tumors. Moreover, the higher microvessel density was consistent with higher tumor weight in parental MS-K tumors.

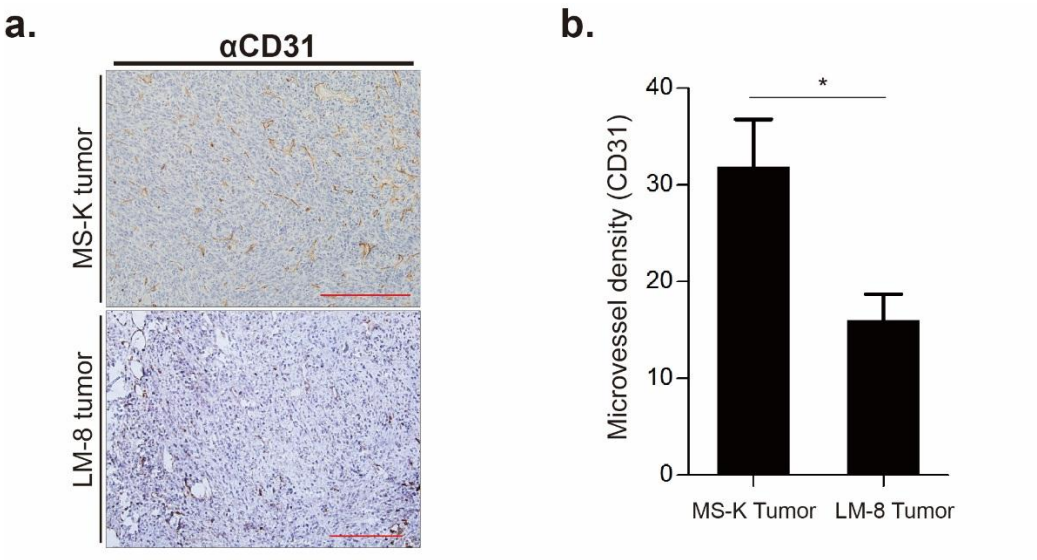

Figure 3. The comparison of MS-K and LM-8 on tumor angiogenesis.

a. Immunohistochemical staining of parental MS-K and parental LM-8 tumor sections was performed using anti-mouse CD31 antibody. The brown area indicates the CD31 positive blood vessels.

b. The microvessel density was calculated in parental MS-K and parental LM-8 tumors by using Image J software. * indicates $p < 0.05$.

3.2 The expression analysis of microRNAs between MS-K and LM-8

Since increasing evidence has shown miRNAs as an important player in tumorigenesis and angiogenesis, we examined several miRNAs' expression between MS-K and LM-8 cell lines. Interestingly, the miR-342 level was found to be approximately 6-fold higher in parental LM-8 cells than parental MS-K cells by quantitative PCR (qPCR) (**Figure 4a**). Furthermore, I confirmed the miR-342 expression in several primary sarcomas. Consistently, qPCR analysis showed that miR-342 was also highly expressed in parental LM-8 tumors compared with parental MS-K tumors (**Figure 4b**). These results indicate inverse correlation of tumor growth, CD31 expression, and miR-342 level in the two-sarcoma cell lines, suggesting a potential regulatory function of miR-342 during tumor progression.

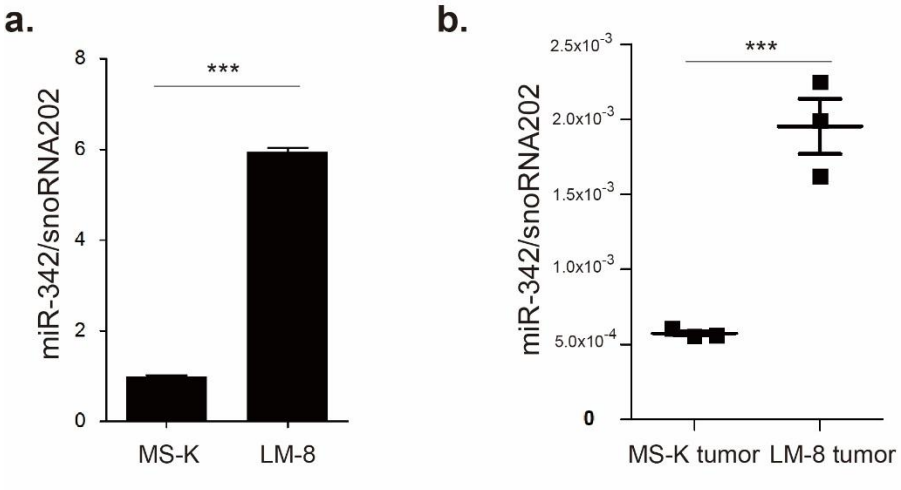

Figure 4. The expression of *miR-342* in parental MS-K and LM-8.

a. The relative expression of miR-342 in parental MS-K and parental LM-8 cell lines by quantitative PCR (qPCR) *in vitro*.

b. The relative expression of miR-342 in tumors (day 22) formed by parental MS-K and parental LM-8 cells by quantitative PCR (qPCR) *in vivo*.

The expression of snoRNA202 was used as a loading control. *** indicates $p < 0.001$.

3.3 The bioinformatics analysis of miRNA-342 sequence

MicroRNAs (miRNAs) are a class of single-strand small noncoding RNAs, composed of ~22 nucleotides, and widely distributed in eukaryotic cells. It is evidence that miRNAs, as a large family of regulatory molecules, have important roles in a wide range of biological processes, including developmental timing, growth control, and differentiation. In animals, miRNAs recognize their target genes mainly through limited base-pairing interactions between the seed sequence of the miRNA (i.e. nucleotides 2-8) and complementary sequence in the 3'-untranslated regions (3'-UTR) of the target mRNAs, resulted in post-transcriptional inhibition of the target mRNAs [10, 61]. MiR-342 is located upstream of *Dlk1-Dio3* imprinted region in mouse chromosome 12. Indeed, recent bioinformatics and experimental evidence indicates that miRNAs within this region have a critical role in tumorigenesis and angiogenesis.

In this study, miR-342 mature sequence was selected as the candidate to investigate its functions and potential molecule mechanisms on tumor growth and blood vessel formation. Firstly, the sequence information and mature sequence conservation were investigated by the bioinformatics. It will be lay the foundation of clarifying its regulatory mechanisms in tumor progression.

The miR-342 gene is embedded, on the sense strand, in the center of a 20.2 kb intron located between the third and fourth exons of the Ena-vasodilator stimulated phosphoprotein (*Evl*) gene on mouse chromosome 12 (**Figure 5**). In addition, the *Evl* gene is located just upstream of the *Dlk1-Dio3* imprinted region. MiR-342 and its host gene *Evl* share a common promotor.

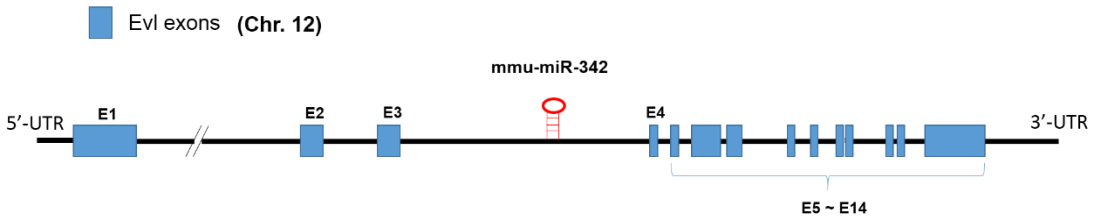

Figure 5. Structure of *Evl* / miR-342 genomic locus on chromosome 12.

Chr. 12: mouse chromosome 12.

Blue box: the exons (exon 1~14) of the gene *Evl*

5'-UTR: 5'- untranslated region; 3'-UTR: 3'- untranslated region.

Mature miR-342 is composed by total 23 nucleotides. MiR-342 is initially transcribed as part of one arm of a ~ 80-nucleotide RNA stem-loop that in turn forms a several hundred nucleotide-long miRNA precursor termed a primary miRNA (pre-miRNA). Then, the pre-miR-342 is cleaved by enzyme Drosha to form pre-miR-342 (precursor-miR-342) (**Figure 6, Upper**). Pre-miR-342 hairpins are exported from the nucleus into the cytoplasm, and cleaved by the RNase III enzyme Dicer, yielding two mature miR-342 from the 3' and 5' arms: (miR-342-3p and miR-342-5p). Although either strand of the duplex may potentially act as a functional miRNA, only one strand is usually incorporated into the RNA-induced silencing complex (RISC) where the miRNA and its mRNA target interact. In this study, we focus on the miR-342-3p, whose relative expression level is higher. More importantly, increasing evidence proved that the regulatory roles of miR-342-3p is involved in cancer.

According to the sequence information from the miRBase database and USCS database, the mature miR-342-3p sequence in mouse share 100% homology with that in rat or human (**Figure 6, Lower**). The 100% sequence homology of homologous miR-342-3p signifies probable functional consistency and regulatory similarity.

Mus musculus pre-miR-342 stem-loop:

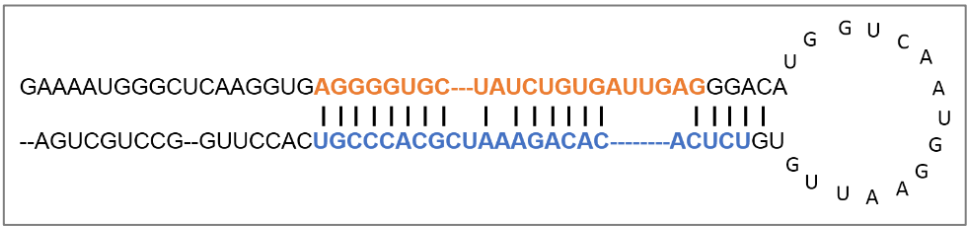

	5’	3’
Mouse	UCUCACACAGAAAUCGCACCCGU	
Human	UCUCACACAGAAAUCGCACCCGU	
Rat	UCUCACACAGAAAUCGCACCCGU	

Figure 6. Analysis of miR-342-3p mature sequence conservation.

Upper: The RNA structure of precursor-miR-342 (mmu-pre-miR-342) stem-loop hairpin.

Lower: The mature sequence alignment of mature miR-342-3p among mouse, rat, and human.

3.4 The establishment of stable miR-342 overexpressing MS-K clones

The miR-342 was found lower expressed in MS-K cells or tumors than that in LM-8 (**Figure 4**). To address the functions miR-342 in tumorigenicity and angiogenesis in MS-K tumors, I stably overexpressed miR-342 in MS-K cells.

At first, the pmR-ZsGreen1-miR-342 vector containing pre-miR-342 fragments or empty vector was constructed. Then, the vectors were transfected into parental MS-K cells, followed by antibiotic selection for 2 weeks. Then, the single cells, with strong green fluorescence protein ZsGreen1 were sorted by a FACSAria II to generate cell clones. Three miR-342 overexpressing MS-K clones (MS-K-miR-342) and control clones (MS-K-mock) were established respectively (**Figure 7**).

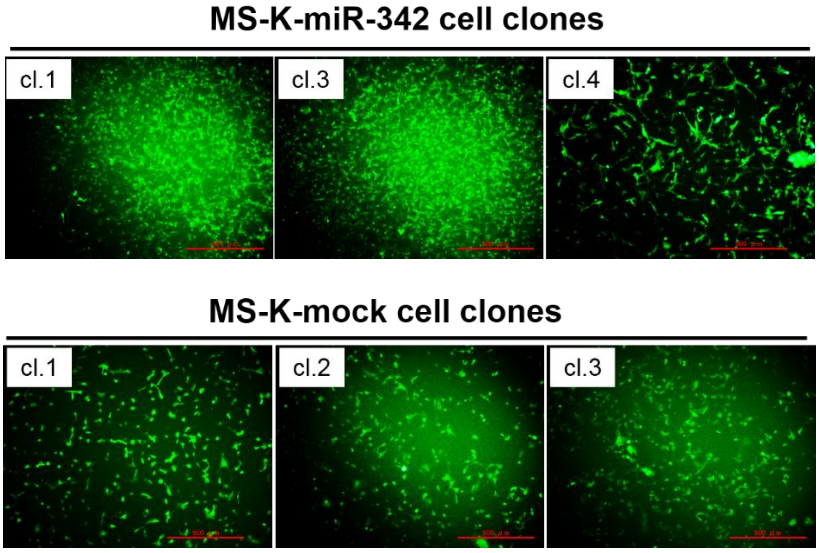

Figure 7. Primary selection of MS-K-miR-342 and MS-K-mock cell clones by fluorescence.

These cell clones were selected by their high expression of fluorescent protein ZsGreen1.

Secondly, the miR-342 level in established cell clones was determined by quantitative PCR (qPCR). QPCR analysis showed that miR-342 expression in all three MS-K-miR-342 clones was higher, compared with MS-K-mock cell clones (**Figure 8**). Especially, in MS-K-miR-342 cl.1 and cl.4, miR-342 level was elevated about three-fold.

On the other hand, I also tried to stable knockdown miR-342 expression by using a CRISPR/Cas9 tool in MS-K cells. The miR-342 seed sequence on genome DNA was successfully mutated, but the miR-342 level was not down-regulated significantly (data not shown).

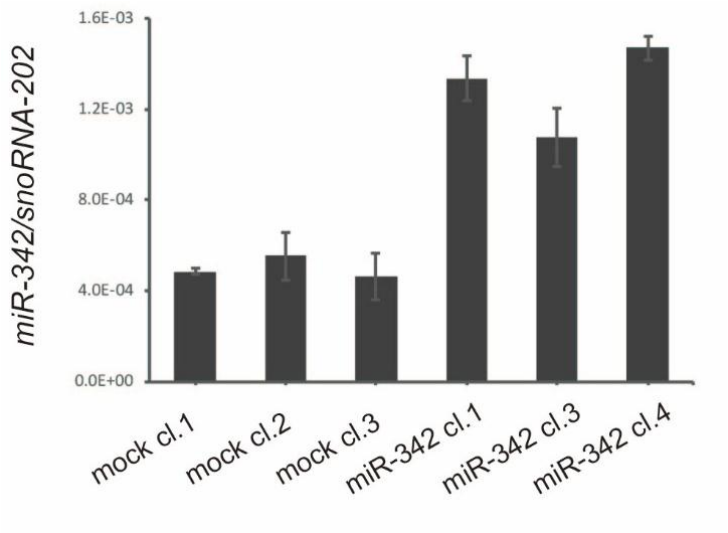

Figure 8. The miR-342 expression in the MS-K-miR-342 clones.

The relative expression of miR-342 (miR-342 / snoRNA202) in the MS-K-miR-342 cell clones was measured by qPCR.

Vascular endothelial growth factor (VEGF) plays a critical role in angiogenesis, which is required for solid tumor growth. Hence, anti-angiogenesis medicine that target the VEGF/VEGF receptor pathway have become a crucial part of standard therapy in multiple cancer indications [62]. Our group has reported that VEGF-A was an indispensable factor for supporting cell proliferation and tumorigenesis of MS-K [63].

Therefore, I examined whether overexpression of miR-342 affects VEGF expression in MS-K cells. RT-PCR was performed to check *Vegf-a, Vegf-c* expression in the MS-K-miR-342 clones. The result showed that both *Vegf-a* and *Vegf-c* were highly expressed either in MS-K-miR-342 cell clones and or in MS-K-mock controls (**Figure 9**). Importantly, the expression of *Vegf-a* or *Vegf-c* was not significantly changed in miR-342-overexpressing MS-K cells contrasted to controls. This result indicates that regulatory functions of miR-342 may not be involved in the VEGF pathway in MS-K.

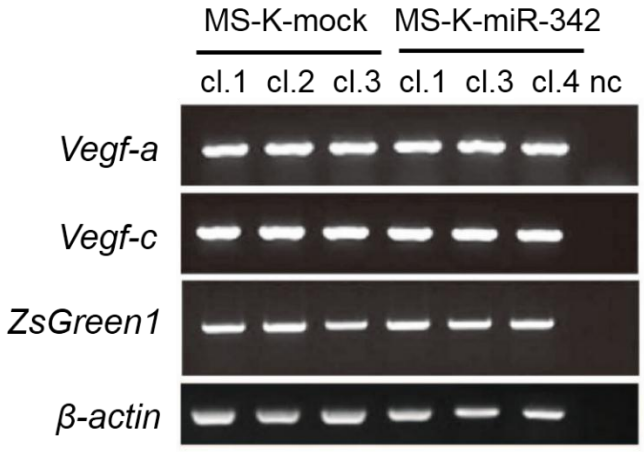

Figure 9. The expression of *Vegf-a*, *Vegf-c* in MS-K-miR-342 clones.

The expression of *Vegf-a*, *Vegf-c*, and *ZsGreen1* in MS-K-miR-342 clones and mock clones was analyzed by RT-PCR. The expression of *β-actin* was used as a loading control.

3.5 The characterization of MS-K-miR-342 clones *in vitro*

In the following, the characteristics of the MS-K-miR-342 clones were investigated *in vitro*.

Firstly, the growth curve assay was carried out and demonstrated that cell growth was decreased in MS-K-miR-342 clones (cl.1, cl.4) compared with MS-K-mock clones (cl.1, cl.2, cl.3) (**Figure 10**).

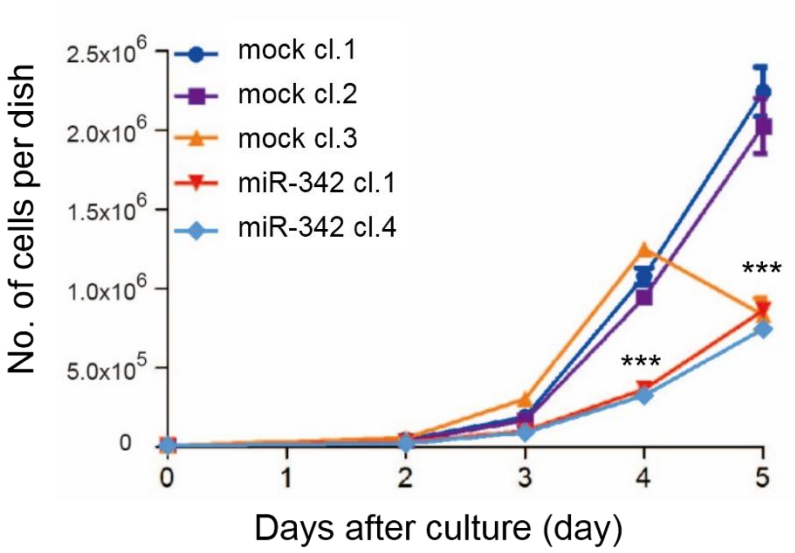

Figure 10. Growth curve of MS-K-miR-342 cell clones *in vitro*.

The living cell number was counted on day 2 to day 5 using Trypan blue staining solution by a hemocytometry. The data indicated mean ± standard deviation (n = 3). *** indicates $p < 0.001$.

Moreover, the colony formation assay showed that enhanced miR-342 levels suppressed colony formation not only in colony numbers but also colony size compared with MS-K-mock clones (**Figure 11**).

These results indicated that miR-342 could inhibit the growth of MS-K cells *in vitro*.

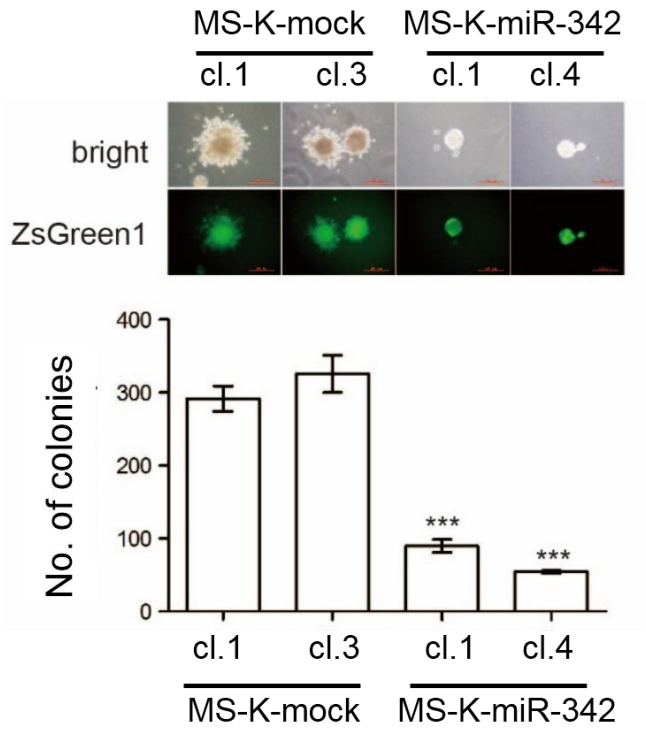

Figure 11. The colony formation assay for MS-K-miR-342 cell clones.

Upper: The photos of the representative colonies of each group were taken on day 17. Lower: The colony numbers were counted on day 17 (diameter > 100 μm). The data indicated mean ± standard deviation (n = 3).

3.5 The effect of miR-342 on cell cycle arrest *in vitro*

Since enhanced miR-342 levels resulted in apparently suppression of MS-K cell proliferation *in vitro* (**Figure 10, 11**), we proceed to investigate potential mechanisms of miR-342-mediated suppression of cell growth. Cell cycle anomalies are often observed in various tumor cells caused by a series of changes in the activity of cell cycle regulators [64, 65]. For instance, inhibitors of the cell cycle keep cells from dividing when conditions are not right, so too little activity of these inhibitors can promote cancer. Similarly, positive regulators of cell division can lead to cancer if they are too active. One of remarkable features of cell cycle of cancer cells is that a normal arrest of cells in G_0/G_1 phase is interrupted, resulted in cell cycle progress into S phase (DNA synthesis

phase) [64]. Here, cell cycle analysis was carried out in cells of parental MS-K, MS-K-mock cl.3 and MS-K-miR-342 cl.4 using Propidium Iodide (PI) staining solution by flow cytometry.

Flow cytometry analysis showed that cell frequency of G_0/G_1 phase of MS-K-miR-342 cl.4 cells was more compared with that in control groups, in contrast, the cell frequency of S phase of MS-K-miR-342 cl.4 cells was lower than controls (**Figure 12**). Further, several cell cycle progression regulatory genes, such as *p21, p27, Cdk2, Cdk2, Cdk6* and *Cyclin D1*, were examined. The RT-PCR result showed that the expression of *p21* and C*dk6* was decreased in MS-K-miR-342 cl.4 cells compared with controls (data not shown). The cyclin kinase inhibitor *p21*, which is a negative regulator of the cell cycle, can induce G_1 arrest and block entry into S phase by inactivating *Cdk2* or by inhibiting activating of proliferating cell nuclear antigen (PCNA) [66]. As well, downregulation of cyclin-dependent kinase 6 (CDK6) can contribute to cell cycle arrest through regulating G_1/S transition and DNA replication [67]. The results indicated that enhanced miR-342 levels could induce cell cycle arrest in G_0/G_1 phase *in vitro*.

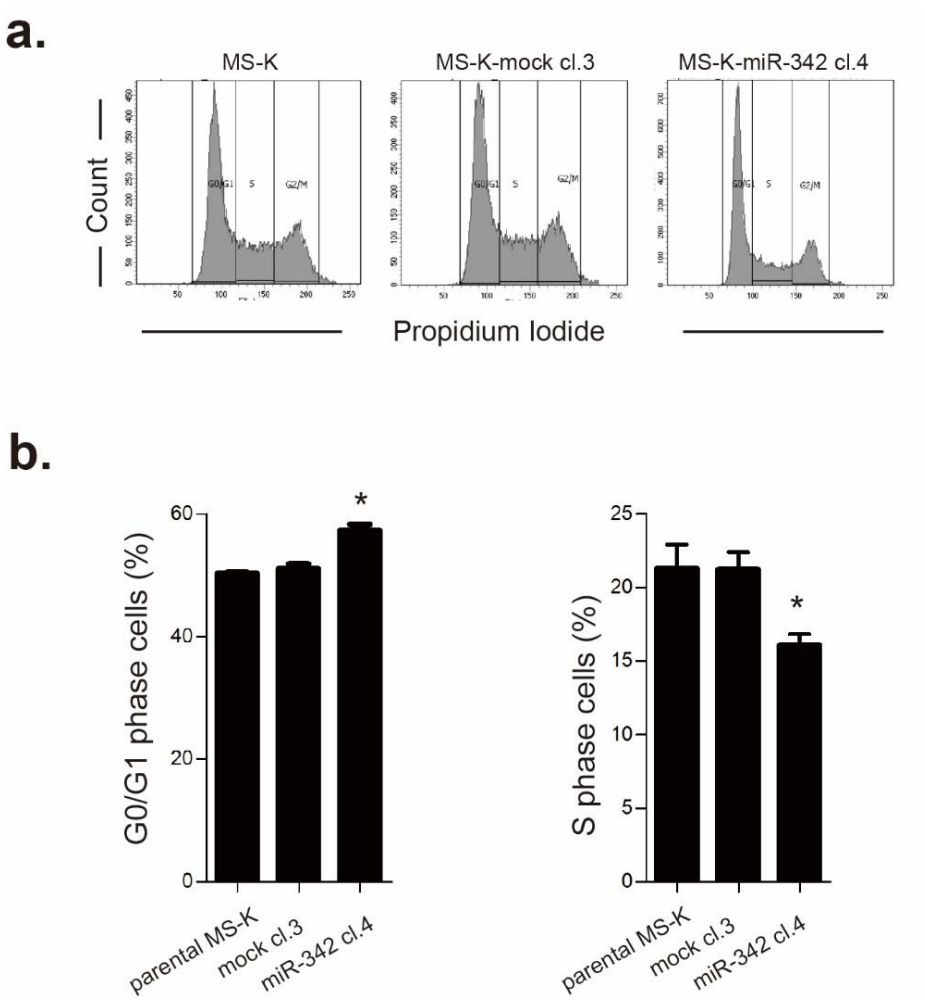

Figure 12. Cell cycle analysis for MS-K-miR-342 cells *in vitro*.

a. Cell cycle assay was performed for parental MS-K, MS-K-mock cl.3 and MS-K-miR-342 cl.4 cells by flow cytometry. The representative plots of each cell group were shown.

b. Cell cycle distributions of parental MS-K, MS-K-mock cl.3 and MS-K-miR-342 cl.4 cells were statistical calculated. The data indicated mean ± standard deviation (n = 3).

3.6 The effect of miR-342 on cell apoptosis *in vitro*

A hallmark of tumor cells is the ability of malignant cells to evade apoptosis [68]. Apoptosis and the genes that control it have a profound effect on the malignant phenotype. To further investigate potential mechanism of suppressive role of miR-342 on cell growth, cell apoptosis assay were carried out in parental MS-K, MS-K-mock cl.3 and MS-K-miR-342 cl.4 cells. The flow cytometry analysis showed that cell apoptosis in MS-K-miR-342 cl.4 was enhanced about 4-fold compared with that in control groups, although apoptosis cells proportion accounted for a fraction of total cells (**Figure 13**). To explore the molecules involved in apoptosis, we measured the expression of p53 in MS-K-miR-342 cell clones. The data showed there was no significantly change of p53 levels (data not shown). Furthermore, we examined the protein-coding sequence of p53 gene by DNA sequencing, but did not observe any mutation (data not shown). Anyway, these results suggest that overexpression of miR-342 could induce apoptosis in MS-K *in vitro*.

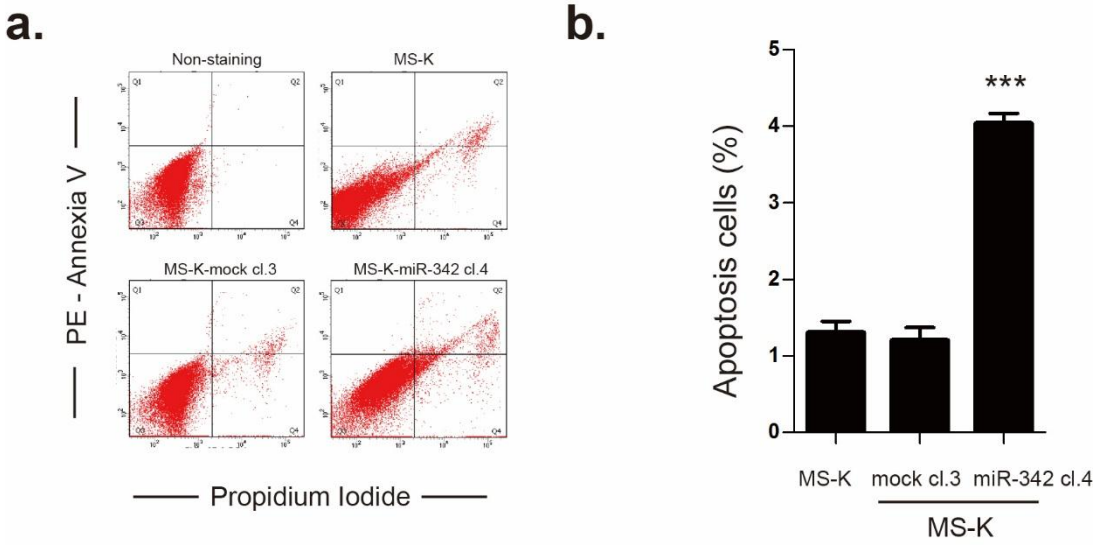

Figure 13. Cell apoptosis analysis for MS-K-miR-342 clone *in vitro*.

a. The representative dot plots of parental MS-K, MS-K-mock cl.3 and MS-K-miR-342 cl.4.

b. The apoptosis cell populations ($PI^-Annexia\ V^+$ and $PI^+Annexia\ V^+$) were calculated and statistical analyzed. The data indicated mean ± standard deviation (n = 3). *** $p<0.001$

3.7 The effect of miR-342 on tumor formation and angiogenesis *in vivo*

Since enhanced miR-342 levels suppressed cell proliferation, induced cell cycle arrest in G_0/G_1 phase and apoptosis in MS-K *in vitro*, we proceeded to investigate its function tumor growth *in vivo*. The cells of MS-K-miR-342 cl.1, cl.4, MS-K-mock cl.1, cl.3 and parental MS-K were used. $1x10^6$ cells were injected subcutaneously into left and right flanks of mammary fat pads of C3H mice. The tumors were allowed to grow over 22 days. At the endpoint, the mice were sacrificed and tumors were excised. From tumors photo, apparent blood vessels could be observed on tumor surface formed by parental MS-K or MS-K-mock clones, in contrast, MS-K-miR-342 tumors showed smaller and less defined blood vessels (**Figure 14a**). The tumor weight was significantly decreased approximately three times for MS-K-miR-342 cl.1 tumors and six times for MS-K-miR-342 cl.4 tumors compared with control groups (**Figure 14b**).

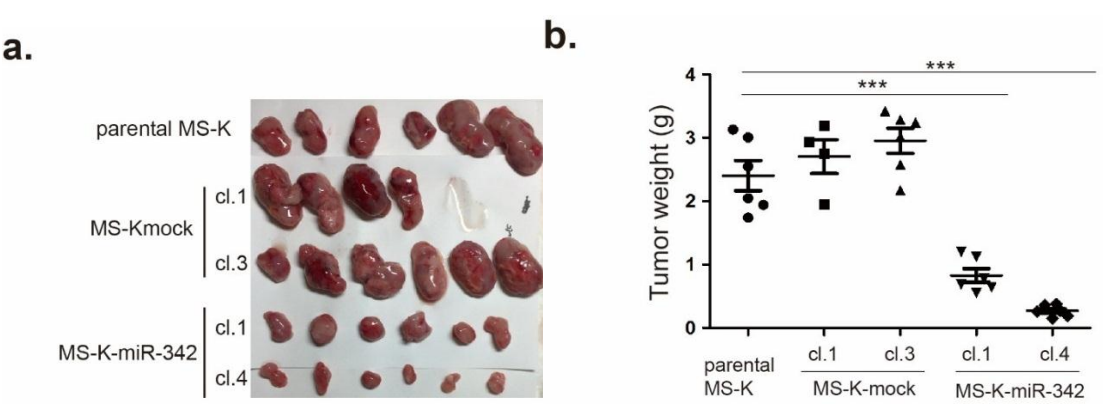

Figure 14. The effect of miR-342 on tumor angiogenesis *in vivo*.

a. The tumor photos formed by parental MS-K, MS-K-mock cl.1, cl.3 and MS-K-miR-342 cl.1, cl.4 (day 22) were taken after tumors excision from C3H mice.

b. The tumor weight were measured and statistical analyzed. The data indicated mean ± standard deviation (n = 4 ~ 6). *** $p < 0.001$

Tumor tissues were fixed and embedded into paraffin blocks. An immunohistochemical staining demonstrated that there was poor blood vessel formation in the MS-K-miR-342 cl.1 and cl.4 tumors, contrary to enriched blood vessels in the parental MS-K tumors or MS-K-mock cl.1, cl.3 tumors (**Figure 15a**). To quantify blood vessel density, the numbers of CD31-positive areas in tumor sections were calculated (**Figure 15b**), indicating a significant decrease in microvessel density in MS-K-miR-342 (cl.1, cl.4) tumors compared with that in controls.

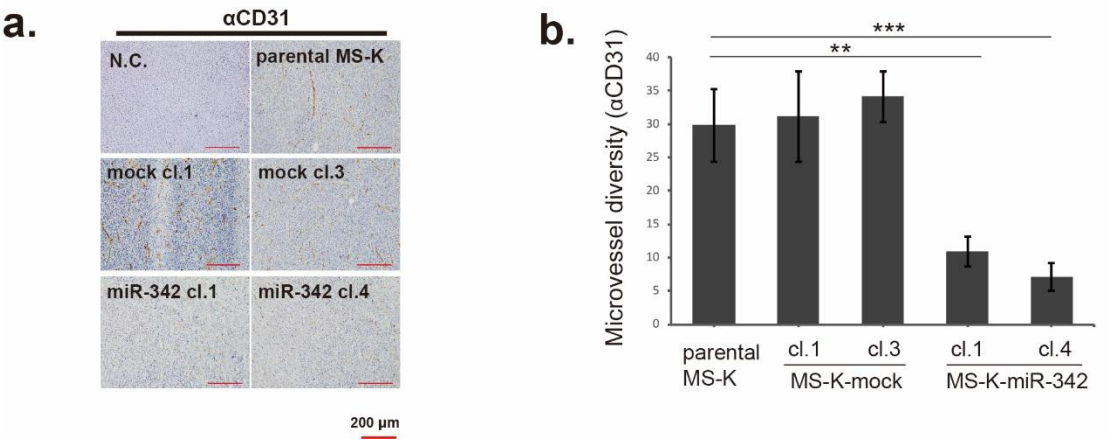

Figure 15. The effect of miR-342 on tumorigenesis *in vivo*.

a. Immunohistochemical staining of parental MS-K, MS-K-mock cl.1, cl.3 and MS-K-miR-342 cl.1, cl.4 tumor sections was performed using anti-CD31 antibody. The brown area means the CD31-positive blood vessels. N.C. indicates negative control, tumor sections without first antibody interaction. Scale bar: 200 μm.

b. The microvessel diversity was calculated in parental MS-K, MS-K-mock cl.1, cl.3 and MS-K-miR-342 cl.1, cl.4 tumors. ** indicates $p < 0.01$ and *** indicates $p < 0.001$.

3.8 The effect of miR-342 on CD11b positive macrophages accumulation

Jeremy J.W. et al. reported that microvessel counts were positively correlated with macrophage density in cancer (Chen et al. 2005). Moreover, our group have previously reported that infiltrated macrophages was a crucial regulator for tumor growth and blood vessel development in MS-K tumor [57, 59]. Therefore, we asked whether enhanced miR-342 levels could affect macrophages accumulation in MS-K tumors.

After tumor excision, some tumors were cut into small pieces and digested into single cells. Then, infiltrated immune cells-macrophages was analyzed by flow cytometry using anti-CD11b antibody (**Figure 16**). The representative flow charts of CD11b+ cells in total tumor cells were presented (**Figure 16a**).The result demonstrated that the ratio of the CD11b-positive cells in the MS-K-miR-342 cl.1 or cl.4 was less than in parental MS-K tumors (**Figure 16b**). Furthermore, the total number of infiltrated CD11b+ cells was also reduced in MS-K-miR-342 cl.1 or cl.4 tumors (**Figure 16c**). Together, these results supported our *in vitro* findings and suggested that macrophages might be involved in mediating the tumor-suppressive functions of miR-342 *in vivo*.

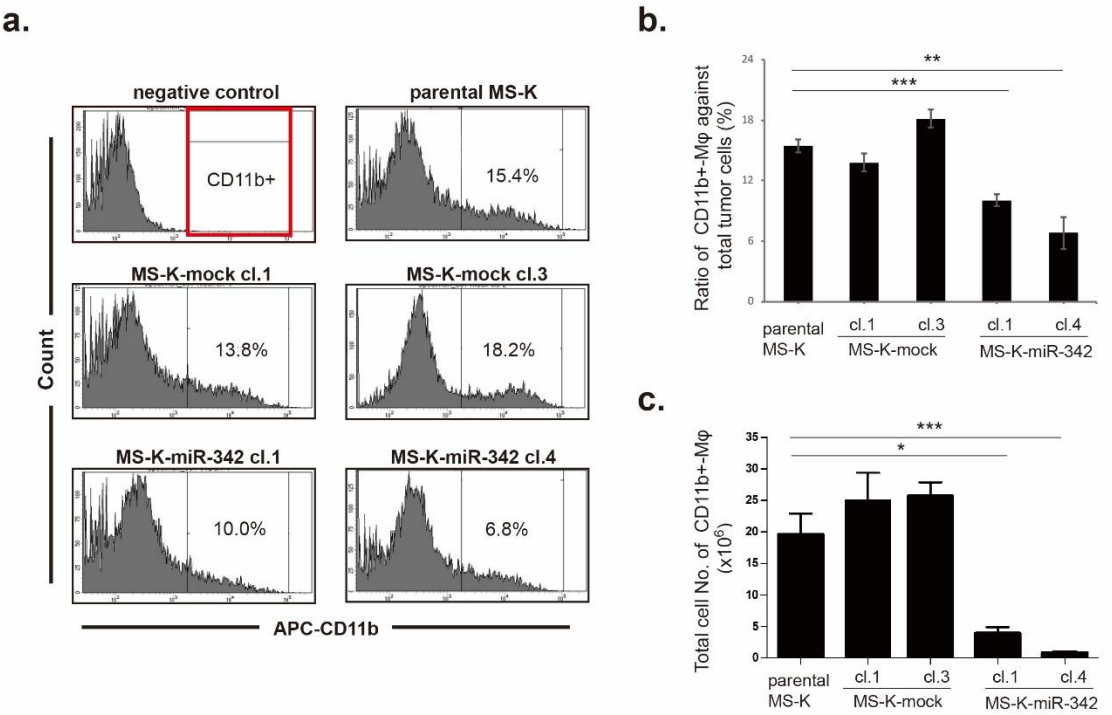

Figure 16. The effect of miR-342 on CD11b-positive cells accumulation.

a. The APC labelled-CD11b-positive cells were analyzed according to the fluorescence of APC. Representative flow of CD11b+ cells in indicated tumors. Numbers indicate mean ratio of the CD11b+ cells against total tumor cells for the group (n = 3).

b. The average percentage of CD11b-positive cells in indicated tumors was statistical calculated (n = 3). ** indicates $p < 0.01$ and *** $p < 0.001$.

c. Total number of infiltrated CD11b-positive cells in indicated tumors was calculated (n = 3). * indicates $p < 0.05$ and *** $p < 0.001$.

3.9 Identification of direct target genes of miR-342

In general, miRNAs regulate protein-coding genes at post-transcriptional level by binding to 3'-untranslated regions on mRNA, resulted in inhibition of translation post-initiation or mRNA degradation [10]. Since miR-342 played a significantly role in cell growth and tumor formation, we performed in silico search for miR-342 targets to clarify the possible molecule mechanism by which miR-342 exerted regulatory role in MS-K.

3.9.1 The bioinformatics prediction of miR-342 target genes

In order to determine the target genes responsible for miR-342-induced suppression of tumor growth, we predicted the target gene of miR-342 *in silico* using three sequence-based target prediction software programs, TargetScan, miRanda and RNA22. Each program yielded a large number of genes as possible miR-342 targets. A candidate gene profile commonly predicted by all of three methods. Macrophages are educated by the cytokine/chemokine milieu in the tumor microenvironment. Various extracellular cytokine/chemokine signals, which recruit and polarize macrophages, have been well-studied [39]. Since miR-342 inhibited regulated tumor growth and macrophage accumulation *in vivo*, it prompted us to focus on predicted cytokine/chemokine genes as possible miR-342 targets. For instance, *Cxcl9, Cxcl10, Cxcl12, Cxcl14, Ccl2, Ccl6* and *Cxcr3*. Among them, chemokine *Cxcl12* was particularly interesting to us because CXCL12, also known as stromal cell-derived factor-1 (SDF-1), drives tumor-associated macrophages accumulation and survival in hypoxic areas of tumors [43]. CXCL12 also displays angiogenic properties via binding to CXCR7 [69, 70] and enhances cell growth by CXCL12/CXCR4 axis in breast cancer and prostate cancer [71, 72]. Moreover, it has been shown that downregulation of CXCL12 resulted in less CXCR4-positive macrophages migration in PDAC [49].

In the following, the expression of these cytokine/chemokine candidates was examined in MS-K-miR-342 cell clones. RT-PCR analysis showed that *Cxcl12* mRNA, together with its receptor *Cxcr7* mRNA, was apparently downregulated in MS-K-miR-342 cl.1, cl.3 and cl.4 compared with that in MS-K-mock cells (**Figure 17a**). However, expression of *Cxcr4*, another receptor of CXCL12, was not detected in any group of cells (data not shown). Then western blot assays showed that CXCL12 protein levels were dramatically decreased in MS-K-miR-342 (cl.1 and cl.4) cells (**Figure 17b**). In addition, we did not detect expression of other predicted candidates, such as *Cxcl9, Cxcl10, Cxcl14, Ccl2, Ccl6* or *Cxcr3*, in any MS-K-miR-342 or MS-K-mock clones (data not shown).

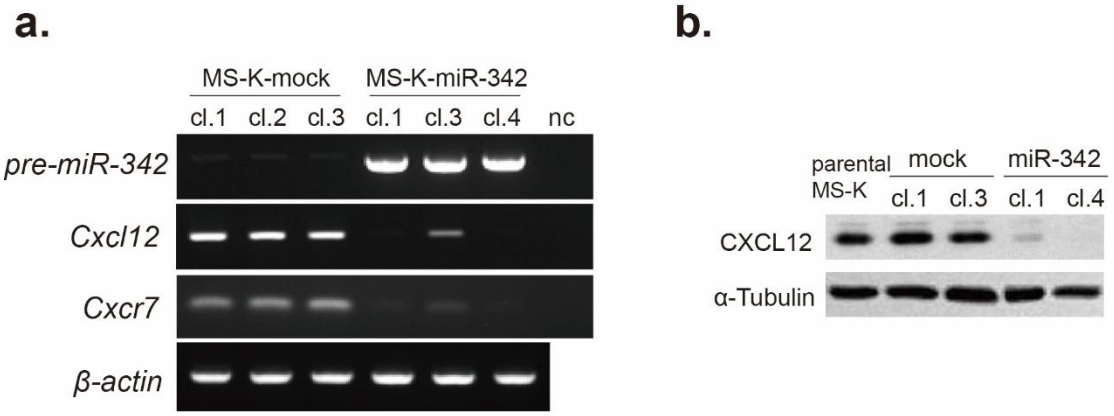

Figure 17. The effect of miR-342 on expression of *Cxcl12* and its receptor.

a. The expression of chemokine *Cxcl12, Cxcr7* and *premiR-342* was analyzed in indicated cell clones by RT-PCR. *β-actin* was used as control.

b. Chemokine CXCL12 protein levels were examined in indicated cell clones by western blot. α-Tubulin was used as control.

3.9.2 The chemokine CXCL12 was a direct target of miR-342

Since chemokine *Cxcl12* was a predicted target of miR-342 and enhanced miR-342 levels down-regulated CXCL12 expression, we proceeded to investigate whether miR-342 repression of *Cxcl12* is mediated by direct interaction of miR-342 with *Cxcl12*-3'UTR by dual-luciferase reporter assay (DLR).

Sequence alignment indicated that miR-342 bound to two sites on 3'UTRs of *Cxcl12* mRNA (407~413 and 1159~1165 base sites, indicated as 3'UTR-wt #1, #2) (**Figure 18a**). Therefore, we amplified two DNA fragments (~300 base pairs) containing the miR-342 binding sites on *Cxcl12* 3'UTRs respectively, and inserted into pMIR-REPORT luciferase vector. The control 3'UTRs fragments were also synthesized where miR-342 binding sequence was mutated, and cloned into the vector.

MS-K-mock cl.3 and MS-K-miR-342 cl.4 cells were transiently transfected with Cxcl12-3'UTRs-wt (#1, #2) or CXCL12-3'UTRs-mut (#1, #2) together with a pRT-TK Renilla vector, which was used as a normalized control. In addition, MS-K-miR-342 cl.4 cells were transiently co-transfected with an empty pMIR-REPORT vector and pRT-TK Renllia vector as a negative control. Forty-eight hours later, the luciferase activity was detected and normalized with Renilla luciferase activity. The DLR assays showed that luciferase activity was significantly decreased in MS-K-miR-342 cells transfected with *Cxcl12*-3'UTR-wt #1, but not mutant *Cxcl12*-3'UTR-mut #1 compared with controls (**Figure 18b**). However, luciferase activity was not changed after transfection with *Cxcl12*-3'UTR-wt #2 or *Cxcl12*-3'UTR-mut #2 in MS-K-miR-342 cells compared with controls (**Figure 18c**). These results suggested that CXCL12 is a direct target of miR-342 in MS-K cells.

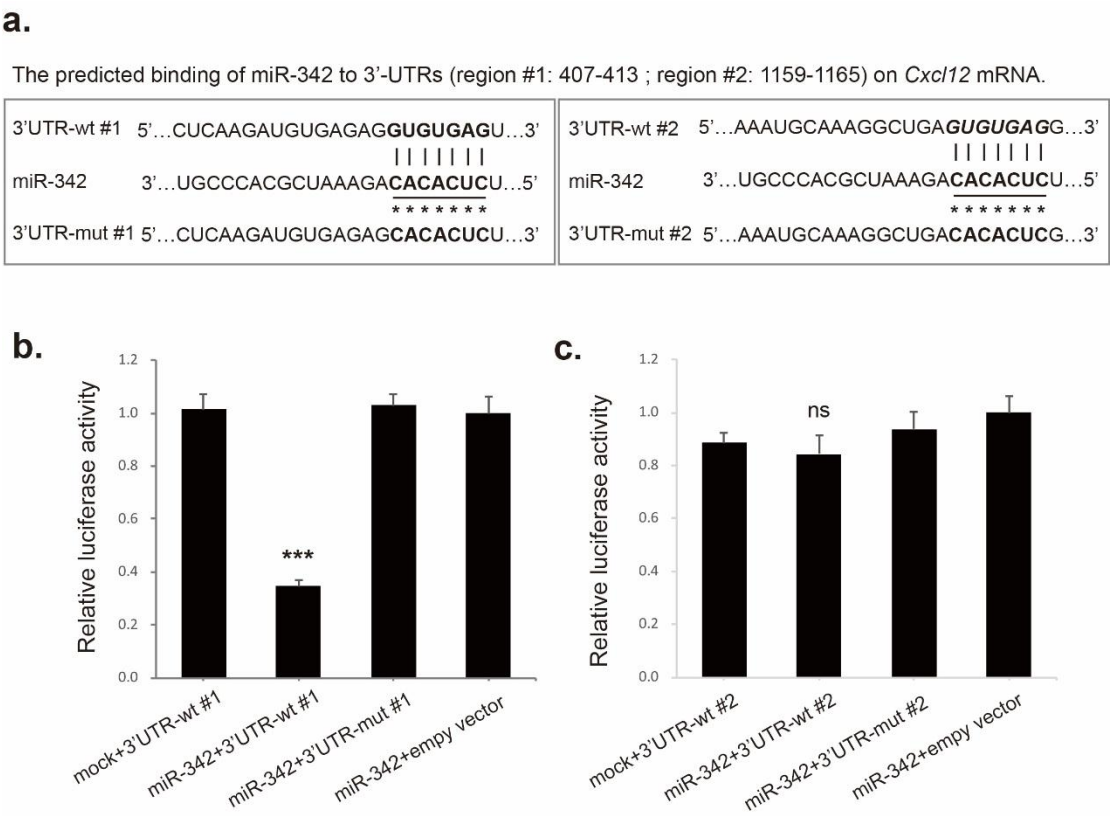

Figure 18. *Cxcl12* is a direct target of miR-342.

a. Computer prediction of the binding of miR-342 to two regions of the CXCL12-3'-UTRs. Sequence alignment of miR-342 and *Cxcl12*-3'-UTRs. Seed sequence of miR-342 are underlined. The mutated base sequences on *Cxcl12*-3'-UTRs are shown with asterisks.

b. Reporter assay was performed in MS-K-miR-342 cl.4 and MS-K-mock cl.3 cells transfected with *Cxcl12*-3'UTR-wt #1 or *Cxcl12*-3'UTR-mut #1.

c. Reporter assay was performed in MS-K-miR-342 cl.4 and MS-K-mock cl.3 cells transfected with *Cxcl12*-3'UTR-wt #2 or *Cxcl12*-3'UTR-mut #2.

Normalized Firefly-luciferase activity (Fluc/Rluc) relative to the control empty pMIR-REPORT vector is shown (n = 3). n.s. indicates non-significant difference. *** indicates $p < 0.001$.

3.10 The effect of miR-342 on macrophages polarization *in vivo*

Chemokine CXCL12 is an important soluble mediator released by malignant cells or tumor stromal cells recruit monocyte/macrophage to the tumor site. CXCL12 also enhances the scavenger receptor CD163 expression, shaping monocyte differentiation toward immunosuppressive phenotype [73]. Since overexpression of miR-342 suppresses macrophages accumulation in MS-K tumor and miR-342 directly targets CXCL12, we next examined if enhanced miR-342 levels could regulate tumor-infiltrated macrophages polarization *in vivo*.

The CD11b-positive cells were isolated from tumors of MS-K-miR-342 (cl.1, cl.4), MS-K-mock (cl.1, cl.3) and parental MS-K using flow cytometry and the RNA was extracted from the cells. The expression of macrophage markers was checked in the tumor derived CD11b-positive cells using qPCR (**Figure 19**). The expression of the M2 macrophage markers (**Figure 19a**), *Cd163, Dectin1* and *Ym1*, was significantly reduced, whereas M1 macrophage marker (**Figure 19b**), Cd80 was increased, in the CD11b+ cells derived from MS-K-miR-342 (cl.1, cl.4) tumors compared with that in control groups. Conversely, the expression of the M2 markers, *Chi3l3* and *il10,* and the M1 marker Cd86 was not affected in the CD11b-positive cells derived from MS-K-miR-342 (cl.1, cl.4) tumors. Moreover, the expressions of M2 markers, *Cd206*, *Arg1* and *Fizz1* was not detected in the CD11b+ cells from any tumors by RT-PCR (data not shown). These results indicated that the miR-342 could suppress M2 macrophage and induce the M1 macrophage in the MS-K tumor.

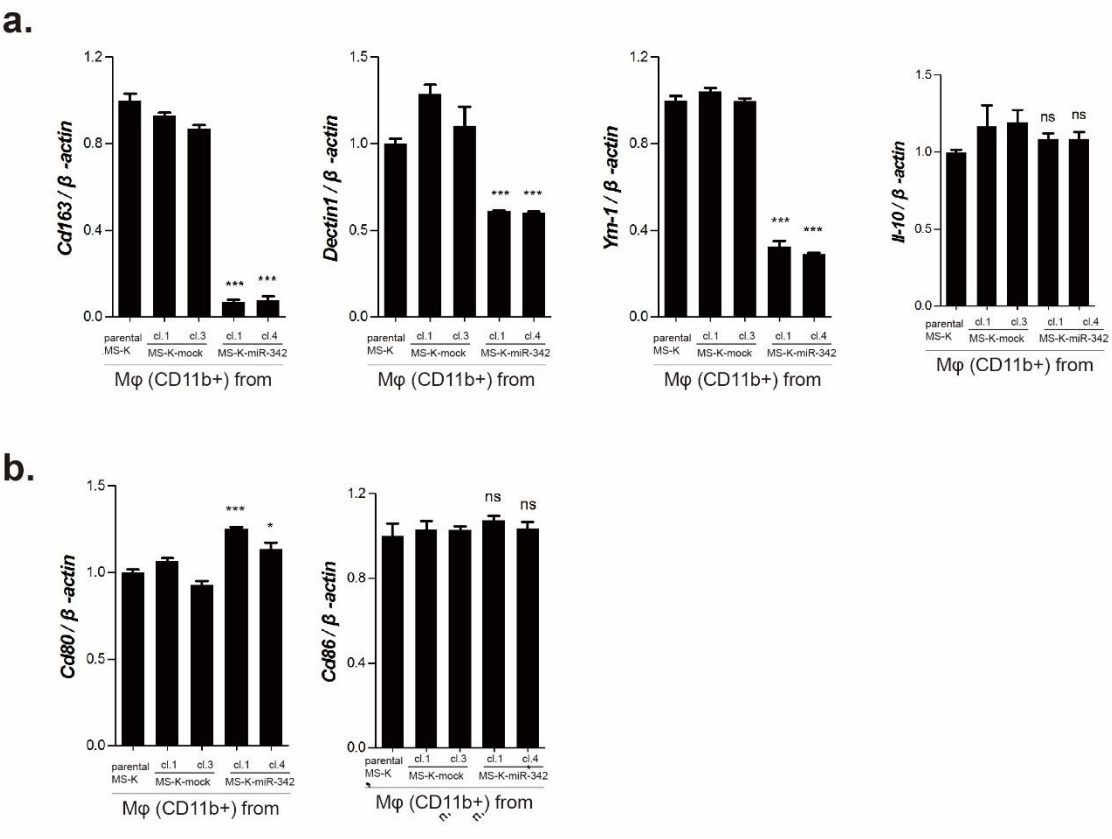

Figure 19. The effect of miR-342 on M2 macrophages polarization.

a. The relative expression of M2 macrophage marker *Cd163, Dectin-1, Ym-1* and *il-10* was analyzed in sorted CD11b-positive cells from indicated tumors by qPCR.

b. The relative expression of M1 macrophage marker *Cd80, Cd86* was analyzed in sorted CD11b-positive cells from indicated tumors by qPCR.

β-actin was used as a loading control. * indicates $p < 0.05$ and *** indicates $p < 0.001$.

3.11 The effect of miR-342 on proangiogenic properties of infiltrated macrophages

Since chemokine CXCL12 enhances VEGF expression and induces macrophages toward to proangiogenic phenotype, we next examined the expression of several proangiogenic genes in the isolated CD11b-positive cells derived from MS-K-miR-342 tumors by qPCR. We found that *Vegf-A* and *Thbs-1* were obviously down-regulated in the CD11b-positive cells of MS-K-miR-342 tumors (cl.1, cl.4) compared with that in control groups (**Figure 20**). These results indicate that infiltrated macrophages in MS-K-miR-342 tumors presented less properties of proangiogenic and cell growth inducible compared with controls.

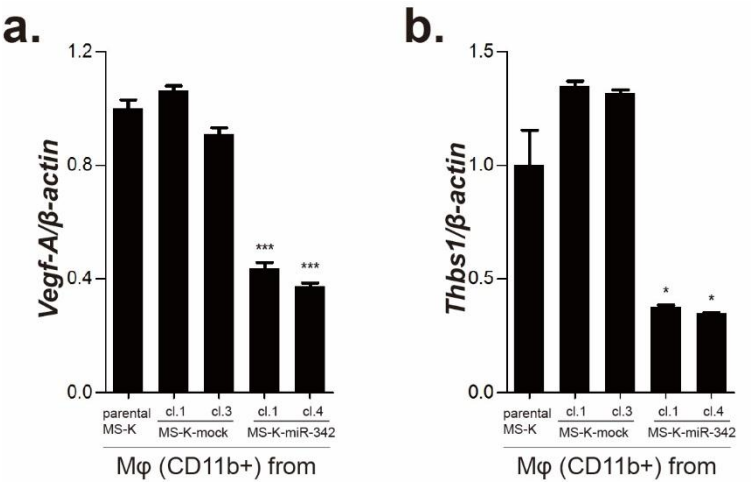

Figure 20. The expression of angiogenic genes in CD11b+ macrophages.

The relative expression of *Vegf-A* (a) and *Thbs-1* (b) was analyzed in sorted CD11b-positive cells from indicated tumors by qPCR. *β-actin* was used as a loading control.

* indicates $p < 0.05$ and *** indicates $p < 0.001$.

3.12 Endogenous miR-342 expression in tumor-infiltrated macrophages

Since miR-342 and its host gene *Evl* share a common promotor, they always present consistently expression pattern. Here, we asked whether overexpression of miR-342 in MS-K could affect the expression of endogenous miR-342 in tumor-infiltrated macrophages. We examined the levels of miR-342 and its host gene, *Evl*, in the CD11b-positive cells derived from MS-K-miR-342 tumors. QPCR analysis showed that miR-342 levels were higher in CD11b+ cells of MS-K-miR-342 tumors (cl.1, cl.4), whereas the expression of *Evl* was not obviously changed (**Figure 21**).

Furthermore, we examined the level of *Cxcl12* and its receptor *Cxcr4* in tumor derived CD11b-positive cells using qPCR. The expressions of *Cxcl12* and *Cxcr4* were lower in the CD11b-positive cells of MS-K-miR-342 tumors (cl.1, cl.4) compared with controls **(Figure 22)**. In addition, the other receptor of CXCL12, *Cxcr7* was not detected in the CD11b+ cells of any tumors by RT-PCR (data not shown).

Taken together, these results indicated that MS-K-miR-342 cells derived miR-342 might be involved in *Cxcl12* inhibition in tumor-infiltrated macrophages, but not endogenous miR-342.

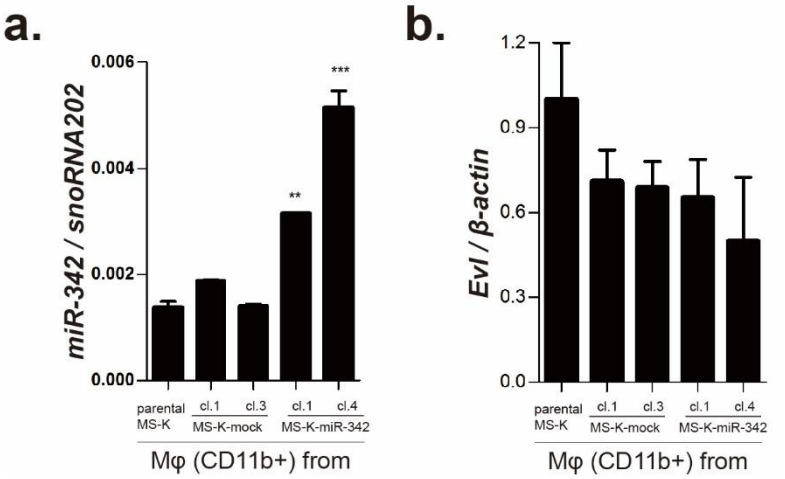

Figure 21. The expression of miR-342 and *Evl* in the CD11b+ macrophages.

The relative expression of *miR-342* (a) and *Evl* (b) was analyzed in sorted CD11b-positive cells from indicated tumors by qPCR. ** indicates $p < 0.01$ and *** indicates $p < 0.001$.

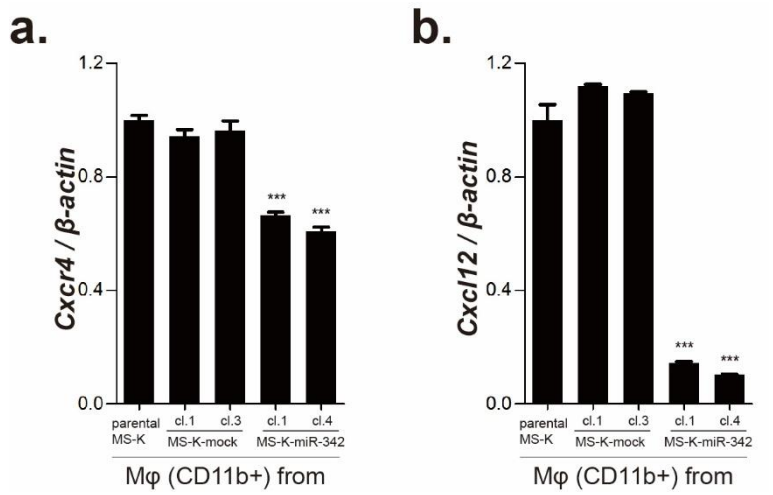

Figure 22. The expression of *Cxcl12, Cxcr4* in the CD11b+ macrophages.

The relative expression of *Cxcr4* (a) and *Cxcl12* (b) was analyzed in sorted CD11b-positive cells from indicated tumors by qPCR. ** indicates $p < 0.01$ and *** indicates $p < 0.001$.

3.13 Introduction of CXCL12 abrogates miR-342 cellular function

3.13.1 Rescue the CXCL12 expression in MS-K-miR-342 cells

Since miR-342 directly targets CXCL12 through interaction between CXCL12 3'UTR and miR-342, I reasoned that ectopic expression of CXCL12 by transfection of the cDNA that only contains the coding region of CXCL12 should escape the regulation by miR-342 and thus attenuate or decrease miR-342 function. To this end, CXCL12 overexpression vector lacking 3'UTR was introduced into miR-342-stable infected MS-K cells. I established four MS-K-miR-342/CXCL12 cell clones. *Cxcl12* expression was confirmed in cell clones, in particular cl. 2, by RT-PCR (**Figure 23**). In addition, the expression of *Cxcl12* receptor, *Cxcr7*, was restored at a certain degree.

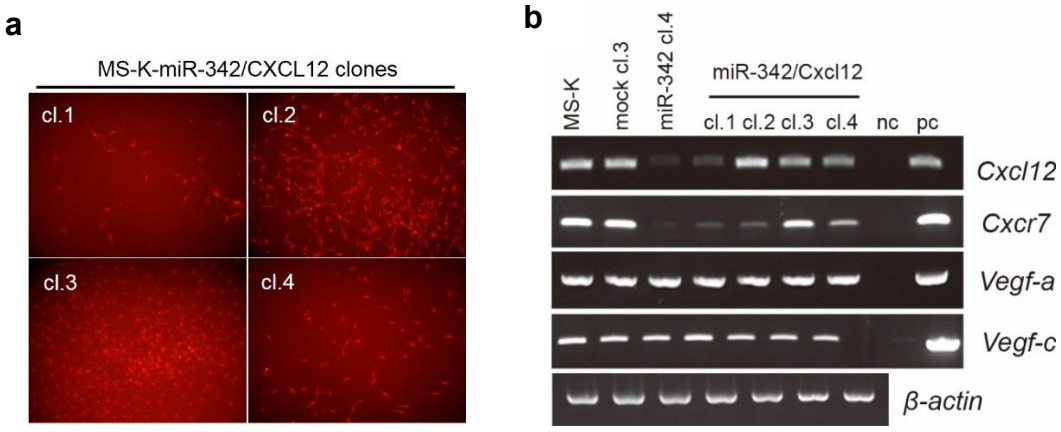

Figure 23. The expression of *Cxcl12, Cxcr7* in MS-K-miR-342/CXCL12 cell clones.

a. Established MS-K-miR-342/Cxcl12 cell clones with Kusabira Orange fluorescence.

b. The expression of *Cxcl12, Cxcr7* and *Vegf-a, Vegf-c, β-actin* was analyzed in parental MS-K, MS-K-mock cl.3, MS-K-miR-342 cl.4 and MS-K-miR-342/CXCL12 cl.1~4 by RT-PCR.

Nc: negative control, pc: positive control.

3.13.2 Rescued CXCL12 attenuated function of miR-342 on cell growth

Growth curve assay showed that there was a significant increase in cell number of MS-K-miR-342/Cxcl12 cl.2, 3, 4 compared with MS-K-miR-342 cells at day 4~5 (**Figure 24**). Further, miR-342-induced G_0/G_1 phase arrest and –reduced S phase were also abrogated by ectopic expression of CXCL12 (supplementary figure S1). Together, CXCL12 could induce cancer cell *in vitro* growth by stimulating DNA synthesis [48]. Based on these results, I conclude that CXCL12 is a major target of miR-342 and largely mediates miR-342 suppressive function in MS-K.

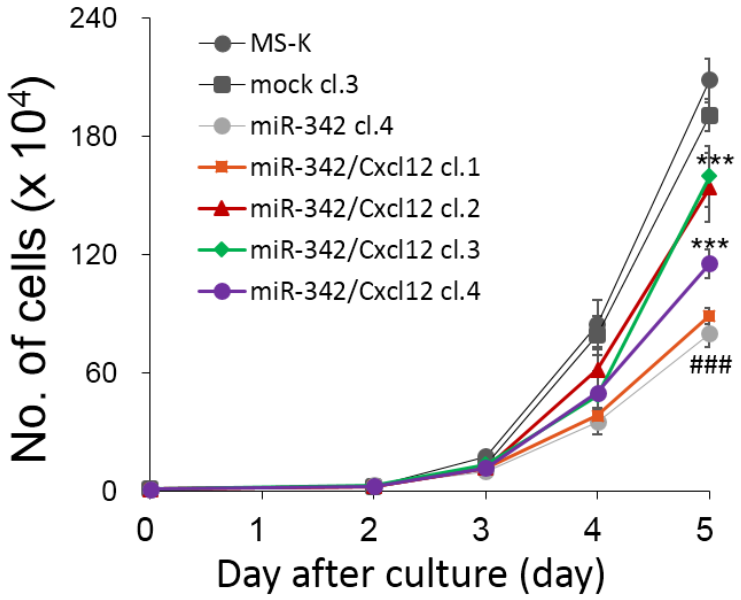

Figure 24. Growth curve of MS-K-miR-342-CXCL12 cell clones *in vitro*.

The living cell number was counted on day 2 ~ 5 using Trypan blue staining solution. The data indicated mean ± standard deviation (n = 3). *** indicates $p < 0.001$.

3.14 Summary

In this study, I found that miR-342 was expressed significantly less in a murine MS-K tumor cell line that showed enriched blood vessels. Overexpressed miR-342 in MS-K inhibited cell proliferation, colony formation, reduced frequency of S phase population *in vitro* and suppressed tumor growth *in vivo*. Moreover, increasing miR-342 impeded blood vessels formation and accumulation of macrophages (CD11b+) in tumors. By bioinformatic analysis and dual-luciferase reporter assays, chemokine CXCL12 was identified as a direct target of miR-342. Restored *Cxcl12* expression in MS-K-miR-342 cells rescued cell proliferation. In MS-K-miR-342 tumor-infiltrated macrophages, proangiogenic genes (*Vegf-A* and *Thbs1*) and M2-subtype macrophage markers (*Cd163, Dectin1* and *Ym1*) was significantly downregulated. Moreover, lower level of *Cxcl12* and its receptor *Cxcr4* was observed in macrophages of MS-K-miR-342 tumors, and MS-K-miR-342 derived miR-342, but not endogenous miR-342, might be contribute to *Cxcl12* suppression in macrophage. These results suggest that miR-342 is involved in tumor growth as a tumor-suppressor by targeting chemokine

CXCL12.

4. Discussion

4.1 MiR-342 was screened as a tumor-regulatory candidate

MicroRNAs (miRNAs) are small RNAs (typically 22 nucleotides in length) that influence gene expression networks by repressing target messenger RNAs [4, 12]. A growing body of literature indicates that miRNAs are dysregulated in malignancies and it has been proposed that some miRNAs may have oncogenic or tumor suppressor functions [15, 74, 75]. Consistent with this idea, both overexpression and silencing of specific miRNA have been described in a number of cancer types. In this study, a comparison of tumor growth indicated that there was significant difference in tumor weight and blood vessel formation between MS-K tumor and LM-8 tumor (**Figure 1, 2**) [76], and miRNAs expression profile analysis showed that the expression of miR-342 was apparently lower expressed in MS-K cells/tumors, where more enriched blood vessel and larger tumors were observed compared with LM-8 tumors (**Figure 3**). These results indicated that miR-342 might affect tumor growth. MiR-342 has been proposed that miR-342 might exert both anti- and pro-tumoral functions based on expression changes and functional analysis [77]. More often, miR-342 was reported to be a tumor-suppressor by down-regulating key oncogenic pathways in various cancers. For instance, miR-342 inhibited proliferation and invasion by targeting RAP2B in non-small lung cancer cell lines [78]. Moreover, miR-342 inhibited the proliferation of HER2-postive breast cancer cells via regulation of the HER2 pathway [79], and inhibited Myc activity by targeting E2F1 in breast cancer cell lines [80]. In colon cancer cell lines, miR-342 has been revealed to be a tumor-suppressor by targeting NAA10 [55] and DNA methyltransferase 1 [52]. Even so, the biological roles and underlying molecular mechanisms of miR-342 in tumorigenesis remain largely unknown.

Therefore, in this study, I focused on miR-342 to try to clarify its detailed function and possible mechanisms in tumor development.

MicroRNA expression is dysregulated in malignancies, frequently leading to loss of expression of certain microRNAs. It was reported that the expression of miR-342 is coordinated with its host gene *Evl,* and down-regulated by CpG island hypermethylation on upstream of *Evl* in human colorectal cancer [50, 51]. I think that the methylation difference of CpG island on *Evl* promotor might be one of important mechanisms resulted in miR-342 silencing between MS-K and LM-8.

4.2 Characteristics of miR-342-overexpressing MS-K cells

Since the expression of miR-342 was lower in MS-K cells compared with LM-8. Thus, I tried to overexpress the miR-342 in the MS-K cells to analyze the role of the miR-342 in cell proliferation and tumorigenesis. The miR-342-overexpressing MS-K cells revealed less proliferation and colony formation ability compared to the mock MS-K cells (**Figure 10, 11**). Furthermore, enhanced miR-342 in MS-K induced cell cycle arrest in G_0/G_1 phase, reduced cell population in S phase (**Figure 12**). These results indicated that miR-342 might affect the cell proliferation *in vitro*. Our group have previously reported that VEGF-A was an indispensable factor for supporting MS-K cell growth [63], however, after overexpression of miR-342, I didn't observed significant changes of *Vegf-A, Vegf-C* levels in MS-K (**Figure 9**). Thus, it suggested that the regulatory mechanism of miR-342 in MS-K was a VEGF-independent manner. I showed that miR-342 directly interacted with 3'-UTR of chemokine CXCL12 and blocked CXCL12 translation (**Figure 17, 18**). It was reported that CXCL12 could induce cancer cell *in vitro* growth by stimulating DNA synthesis [48]. Hereby, suppressive role of miR-342 might be mediated by down-regulating chemokine CXCL12 regulation in MS-K cells proliferation *in vitro*.

The MS-K-miR-342 tumors weight was reduced significantly *in vivo*, and enhanced miR-342 resulted in blood vessel formation inhibition (**Figure 14, 15**). These findings were further demonstrated the functional effect of miR-342 as a novel tumor suppressor in MS-K. Interestingly, in MS-K-miR-342 tumors, decreased CD11b-positive macrophages accumulation was observed compared with control groups (**Figure 16**). Tumor-associated macrophages (TAM) are a major type of infiltrating immune cells and are critical regulators of the balance between inflammation and cancer [39, 81]. Moreover, chemokine CXCL12 is one of main extracellular signals which recruit M2 or M2-like tumor-associated macrophages by CXCL12/CXCR4 axis [39].

Furthermore, ectopic expression of CXCL12 by transfection of the cDNA that only contains the coding region of CXCL12 attenuated the miR-342 function on cell proliferation (**Figure 24**). Taken together, these results suggest that miR-342 is a tumor-suppressor, mediated not only by impairing proliferative activity of MS-K cells, but also by affecting macrophages accumulation in tumor.

In addition, loss of function of miR-342 is also an important way for studying its functions on tumor growth. In this study, I also tried to knockout miR-342 from genome DNA using CRISPR/Cas9 system. Although, I successfully made mutation of miR-342 locus on genome DNA, decreased miR-342 level was not observed in MS-K cells. The effect of knockdown of miR-342 on tumor growth needs to be addressed in further studies.

4.3 Effect of miR-342 on properties of tumor-infiltrated macrophages

Tumor-associated macrophages (TAMs) can be induced by various extracellular signals in the tumor microenvironment to acquire the hallmarks of alternatively activated M2 macrophages. It was reported that CXCL12 drive TAM infiltration and survival under hypoxic conditions in tumors [43], and induce expression of CD163 and VEGF, shaping monocyte differentiation toward a

proangiogenic and immunosuppressive phenotype [73]. In MS-K tumors, our group have reported previously the function of IL-18-induced activation of macrophages on repression of blood vessel formation [57]. Thus, I further evaluated the properties of infiltrated macrophages in MS-K-miR-342 tumors by determining gene expression in the current study. Proangiogenic factors, such as *Vegf-A* and *Thbs1*, were found to be expressed less in the CD11b-positive cells derived from MS-K-miR-342 tumors (**Figure 20**). Furthermore, the expression of M2 macrophage markers, *Cd163, Dectin1* and *Ym1* were decreased, inversely, the M1 macrophage marker, *Cd80* was increased, in the CD11b-positive cells derived from MS-K-miR-342 tumors compared with controls (**Figure 19**). Taken together, these findings indicated that miR-342 destroyed tumor growth by suppressed the polarization of M2 type macrophages *in vivo*, and the mechanism by which miR-342 affected macrophages polarization might be mediated by downregulation of chemokine CXCL12.

4.4 Endogenous miR-342 expression in tumor-infiltrated macrophages

Increasing studies pay attention to the effects of key miRNAs on monocyte/macrophage lineage development and on the polarization of TAMs. For instance, miR-146a controls the expansion and recruitment of inflammatory monocyte precursors by targeting Relb and CCR2 in the $Ly6C^{high}$ subset in a *Lis-teria monocytogenes* infection model [82]. In bone marrow-derived macrophages (BMDMs), M1 polarization by LPS/IFN-γ induced miR-155, while M2 polarization by IL-4 induced miR-146a [83]. Macrophages miRNA profile are also a characteristic of macrophage polarization. Moreover, IL-4/STAT6-regulated miR-342 plays a pro-apoptosis role in alternatively activated human and mouse macrophages [84]. In this study, I found that the expression of miR-342 was increased in the CD11b-positive cells derived from MS-K-miR-342

tumors, whereas the level of its host gene, *Evl*, was not significantly changed (**Figure 21**). Moreover, I detected the expression of exosome markers, *Cd9*, *Cd63* and *Cd81* by RT-PCR in MS-K cells (data not shown). These data suggest that increased miR-342 levels was due to MS-K cells derived miR-342, but not endogenous miR-342. In another word, exosome mediated miR-342 transportation might be the manner contributed to increased miR-342 levels in tumor-infiltrated macrophage. In addition, the expression of *Cxcl12* and *Cxcr4* was down-regulated in the CD11b-positive cells derived from MS-K-miR-342 tumors compared with control groups (**Figure 20**). Thus, I speculate that miR-342 could directly regulates macrophages viability and/or polarization via targeting CXCL12 in tumor-infiltrated macrophages in MS-K tumor.

4.5 Conclusion

In conclusion, this study investigated the functional role of miR-342 in tumorigenesis and its potential molecular mechanisms. MiR-342 was screened and experimental proved as a tumor suppressor in MS-K. Enhanced miR-342 level impaired cell proliferative activity in MS-K cells. Chemokine CXCL12 was a new direct target of miR-342 and negatively regulated by miR-342, and mediated miR-342 function in the MS-K cell proliferation and growth. Inhibition of macrophages accumulation and M2 macrophage polarization by miR-342 downregulated CXCL12 impeded tumor growth and blood vessel development *in vivo*.

These results suggested the tumor-suppressive capacity of miR-342 in tumorigenesis via targeting chemokine CXCL12 involved in macrophages accumulation/activation, indicating a therapeutic target in the solid tumor intervention.

References

1. Bartel DP: **MicroRNAs: genomics, biogenesis, mechanism, and function**. *Cell* 2004, **116**(2):281-297.
2. Ambros V: **MicroRNA pathways in flies and worms: growth, death, fat, stress, and timing**. *Cell* 2003, **113**(6):673-676.
3. Delay C, Mandemakers W, Hebert SS: **MicroRNAs in Alzheimer's disease**. *Neurobiology of disease* 2012, **46**(2):285-290.
4. Lee Y, Kim M, Han J, Yeom KH, Lee S, Baek SH, Kim VN: **MicroRNA genes are transcribed by RNA polymerase II**. *The EMBO journal* 2004, **23**(20):4051-4060.
5. Yi R, Qin Y, Macara IG, Cullen BR: **Exportin-5 mediates the nuclear export of pre-microRNAs and short hairpin RNAs**. *Genes & development* 2003, **17**(24):3011-3016.
6. Bhayani MK, Calin GA, Lai SY: **Functional relevance of miRNA sequences in human disease**. *Mutation research* 2012, **731**(1-2):14-19.
7. Eulalio A, Huntzinger E, Nishihara T, Rehwinkel J, Fauser M, Izaurralde E: **Deadenylation is a widespread effect of miRNA regulation**. *Rna* 2009, **15**(1):21-32.
8. Bushati N, Cohen SM: **microRNA functions**. *Annual review of cell and developmental biology* 2007, **23**:175-205.
9. Eulalio A, Huntzinger E, Izaurralde E: **Getting to the root of miRNA-mediated gene silencing**. *Cell* 2008, **132**(1):9-14.
10. Nilsen TW: **Mechanisms of microRNA-mediated gene regulation in animal cells**. *Trends in genetics : TIG* 2007, **23**(5):243-249.
11. Peters L, Meister G: **Argonaute proteins: mediators of RNA silencing**. *Molecular cell* 2007, **26**(5):611-623.
12. Meister G: **miRNAs get an early start on translational silencing**. *Cell* 2007, **131**(1):25-28.
13. Baek D, Villen J, Shin C, Camargo FD, Gygi SP, Bartel DP: **The impact of microRNAs on protein output**. *Nature* 2008, **455**(7209):64-71.
14. Selbach M, Schwanhausser B, Thierfelder N, Fang Z, Khanin R, Rajewsky N: **Widespread changes in protein synthesis induced by microRNAs**. *Nature* 2008,

455(7209):58-63.

15. Iorio MV, Croce CM: **MicroRNA dysregulation in cancer: diagnostics, monitoring and therapeutics. A comprehensive review**. *EMBO molecular medicine* 2012, **4**(3):143-159.

16. Calin GA, Dumitru CD, Shimizu M, Bichi R, Zupo S, Noch E, Aldler H, Rattan S, Keating M, Rai K *et al*: **Frequent deletions and down-regulation of micro- RNA genes miR15 and miR16 at 13q14 in chronic lymphocytic leukemia**. *Proceedings of the National Academy of Sciences of the United States of America* 2002, **99**(24):15524-15529.

17. Cimmino A, Calin GA, Fabbri M, Iorio MV, Ferracin M, Shimizu M, Wojcik SE, Aqeilan RI, Zupo S, Dono M *et al*: **miR-15 and miR-16 induce apoptosis by targeting BCL2**. *Proceedings of the National Academy of Sciences of the United States of America* 2005, **102**(39):13944-13949.

18. Johnson SM, Grosshans H, Shingara J, Byrom M, Jarvis R, Cheng A, Labourier E, Reinert KL, Brown D, Slack FJ: **RAS is regulated by the let-7 microRNA family**. *Cell* 2005, **120**(5):635-647.

19. Garzon R, Heaphy CE, Havelange V, Fabbri M, Volinia S, Tsao T, Zanesi N, Kornblau SM, Marcucci G, Calin GA *et al*: **MicroRNA 29b functions in acute myeloid leukemia**. *Blood* 2009, **114**(26):5331-5341.

20. Mott JL, Kobayashi S, Bronk SF, Gores GJ: **mir-29 regulates Mcl-1 protein expression and apoptosis**. *Oncogene* 2007, **26**(42):6133-6140.

21. Sampson VB, Rong NH, Han J, Yang Q, Aris V, Soteropoulos P, Petrelli NJ, Dunn SP, Krueger LJ: **MicroRNA let-7a down-regulates MYC and reverts MYC-induced growth in Burkitt lymphoma cells**. *Cancer research* 2007, **67**(20):9762-9770.

22. Iorio MV, Ferracin M, Liu CG, Veronese A, Spizzo R, Sabbioni S, Magri E, Pedriali M, Fabbri M, Campiglio M *et al*: **MicroRNA gene expression deregulation in human breast cancer**. *Cancer research* 2005, **65**(16):7065-7070.

23. Ciafre SA, Galardi S, Mangiola A, Ferracin M, Liu CG, Sabatino G, Negrini M, Maira G, Croce CM, Farace MG: **Extensive modulation of a set of microRNAs in primary glioblastoma**. *Biochemical and biophysical research communications* 2005,

334(4):1351-1358.

24. Bloomston M, Frankel WL, Petrocca F, Volinia S, Alder H, Hagan JP, Liu CG, Bhatt D, Taccioli C, Croce CM: **MicroRNA expression patterns to differentiate pancreatic adenocarcinoma from normal pancreas and chronic pancreatitis**. *Jama* 2007, **297**(17):1901-1908.

25. Schetter AJ, Leung SY, Sohn JJ, Zanetti KA, Bowman ED, Yanaihara N, Yuen ST, Chan TL, Kwong DL, Au GK *et al*: **MicroRNA expression profiles associated with prognosis and therapeutic outcome in colon adenocarcinoma**. *Jama* 2008, **299**(4):425-436.

26. Frankel LB, Christoffersen NR, Jacobsen A, Lindow M, Krogh A, Lund AH: **Programmed cell death 4 (PDCD4) is an important functional target of the microRNA miR-21 in breast cancer cells**. *The Journal of biological chemistry* 2008, **283**(2):1026-1033.

27. Meng F, Henson R, Wehbe-Janek H, Ghoshal K, Jacob ST, Patel T: **MicroRNA-21 regulates expression of the PTEN tumor suppressor gene in human hepatocellular cancer**. *Gastroenterology* 2007, **133**(2):647-658.

28. Medina PP, Nolde M, Slack FJ: **OncomiR addiction in an in vivo model of microRNA-21-induced pre-B-cell lymphoma**. *Nature* 2010, **467**(7311):86-90.

29. Garzon R, Volinia S, Liu CG, Fernandez-Cymering C, Palumbo T, Pichiorri F, Fabbri M, Coombes K, Alder H, Nakamura T *et al*: **MicroRNA signatures associated with cytogenetics and prognosis in acute myeloid leukemia**. *Blood* 2008, **111**(6):3183-3189.

30. He L, Thomson JM, Hemann MT, Hernando-Monge E, Mu D, Goodson S, Powers S, Cordon-Cardo C, Lowe SW, Hannon GJ *et al*: **A microRNA polycistron as a potential human oncogene**. *Nature* 2005, **435**(7043):828-833.

31. Xiao C, Srinivasan L, Calado DP, Patterson HC, Zhang B, Wang J, Henderson JM, Kutok JL, Rajewsky K: **Lymphoproliferative disease and autoimmunity in mice with increased miR-17-92 expression in lymphocytes**. *Nature immunology* 2008, **9**(4):405-414.

32. Mu P, Han YC, Betel D, Yao E, Squatrito M, Ogrodowski P, de Stanchina E, D'Andrea

A, Sander C, Ventura A: **Genetic dissection of the miR-17~92 cluster of microRNAs in Myc-induced B-cell lymphomas**. *Genes & development* 2009, **23**(24):2806-2811.

33. Kim J, Bae JS: **Tumor-Associated Macrophages and Neutrophils in Tumor Microenvironment**. *Mediators of inflammation* 2016, **2016**:6058147.

34. Robinson BD, Sica GL, Liu YF, Rohan TE, Gertler FB, Condeelis JS, Jones JG: **Tumor microenvironment of metastasis in human breast carcinoma: a potential prognostic marker linked to hematogenous dissemination**. *Clinical cancer research : an official journal of the American Association for Cancer Research* 2009, **15**(7):2433-2441.

35. Sica A, Erreni M, Allavena P, Porta C: **Macrophage polarization in pathology**. *Cellular and molecular life sciences : CMLS* 2015, **72**(21):4111-4126.

36. Gordon S: **Alternative activation of macrophages**. *Nature reviews Immunology* 2003, **3**(1):23-35.

37. Mantovani A, Sozzani S, Locati M, Allavena P, Sica A: **Macrophage polarization: tumor-associated macrophages as a paradigm for polarized M2 mononuclear phagocytes**. *Trends in immunology* 2002, **23**(11):549-555.

38. Allavena P, Sica A, Solinas G, Porta C, Mantovani A: **The inflammatory micro-environment in tumor progression: the role of tumor-associated macrophages**. *Critical reviews in oncology/hematology* 2008, **66**(1):1-9.

39. Szebeni GJ, Vizler C, Kitajka K, Puskas LG: **Inflammation and Cancer: Extra- and Intracellular Determinants of Tumor-Associated Macrophages as Tumor Promoters**. *Mediators of inflammation* 2017, **2017**:9294018.

40. Biswas SK, Allavena P, Mantovani A: **Tumor-associated macrophages: functional diversity, clinical significance, and open questions**. *Seminars in immunopathology* 2013, **35**(5):585-600.

41. Porta C, Riboldi E, Ippolito A, Sica A: **Molecular and epigenetic basis of macrophage polarized activation**. *Seminars in immunology* 2015, **27**(4):237-248.

42. De Vlaeminck Y, Gonzalez-Rascon A, Goyvaerts C, Breckpot K: **Cancer-Associated Myeloid Regulatory Cells**. *Frontiers in immunology* 2016, **7**:113.

43. Wang SC, Hong JH, Hsueh C, Chiang CS: **Tumor-secreted SDF-1 promotes glioma**

invasiveness and TAM tropism toward hypoxia in a murine astrocytoma model. *Laboratory investigation; a journal of technical methods and pathology* 2012, **92**(1):151-162.

44. Teicher BA, Fricker SP: **CXCL12 (SDF-1)/CXCR4 pathway in cancer**. *Clinical cancer research : an official journal of the American Association for Cancer Research* 2010, **16**(11):2927-2931.

45. Lv Y, Lei Y, Hu Y, Ding W, Zhang C, Fang C: **miR-448 negatively regulates ovarian cancer cell growth and metastasis by targeting CXCL12**. *Clinical & translational oncology : official publication of the Federation of Spanish Oncology Societies and of the National Cancer Institute of Mexico* 2015, **17**(11):903-909.

46. Dong S, Jin M, Li Y, Ren P, Liu J: **MiR-137 acts as a tumor suppressor in papillary thyroid carcinoma by targeting CXCL12**. *Oncology reports* 2016, **35**(4):2151-2158.

47. Zhang J, Liu J, Liu Y, Wu W, Li X, Wu Y, Chen H, Zhang K, Gu L: **miR-101 represses lung cancer by inhibiting interaction of fibroblasts and cancer cells by down-regulating CXCL12**. *Biomedicine & pharmacotherapy = Biomedecine & pharmacotherapie* 2015, **74**:215-221.

48. Scotton CJ, Wilson JL, Scott K, Stamp G, Wilbanks GD, Fricker S, Bridger G, Balkwill FR: **Multiple actions of the chemokine CXCL12 on epithelial tumor cells in human ovarian cancer**. *Cancer research* 2002, **62**(20):5930-5938.

49. Fan Y, Xu LL, Shi CY, Wei W, Wang DS, Cai DF: **MicroRNA-454 regulates stromal cell derived factor-1 in the control of the growth of pancreatic ductal adenocarcinoma**. *Scientific reports* 2016, **6**:22793.

50. Seitz H, Royo H, Bortolin ML, Lin SP, Ferguson-Smith AC, Cavaille J: **A large imprinted microRNA gene cluster at the mouse Dlk1-Gtl2 domain**. *Genome research* 2004, **14**(9):1741-1748.

51. Grady WM, Parkin RK, Mitchell PS, Lee JH, Kim YH, Tsuchiya KD, Washington MK, Paraskeva C, Willson JK, Kaz AM *et al*: **Epigenetic silencing of the intronic microRNA hsa-miR-342 and its host gene EVL in colorectal cancer**. *Oncogene* 2008, **27**(27):3880-3888.

52. Wang H, Wu J, Meng X, Ying X, Zuo Y, Liu R, Pan Z, Kang T, Huang W: **MicroRNA-**

342 inhibits colorectal cancer cell proliferation and invasion by directly targeting DNA methyltransferase 1. *Carcinogenesis* 2011, **32**(7):1033-1042.

53. Tai MC, Kajino T, Nakatochi M, Arima C, Shimada Y, Suzuki M, Miyoshi H, Yatabe Y, Yanagisawa K, Takahashi T: **miR-342-3p regulates MYC transcriptional activity via direct repression of E2F1 in human lung cancer**. *Carcinogenesis* 2015.

54. Yang H, Li Q, Niu J, Li B, Jiang D, Wan Z, Yang Q, Jiang F, Wei P, Bai S: **microRNA-342-5p and miR-608 inhibit colon cancer tumorigenesis by targeting NAA10**. *Oncotarget* 2015.

55. Yang H, Li Q, Niu J, Li B, Jiang D, Wan Z, Yang Q, Jiang F, Wei P, Bai S: **microRNA-342-5p and miR-608 inhibit colon cancer tumorigenesis by targeting NAA10**. *Oncotarget* 2016, **7**(3):2709-2720.

56. Cui W, Huang Z, He H, Gu N, Qin G, Lv J, Zheng T, Sugimoto K, Wu Q: **MiR-1188 at the imprinted Dlk1-Dio3 domain acts as a tumor suppressor in hepatoma cells**. *Molecular biology of the cell* 2015, **26**(8):1416-1427.

57. Xing Y, Tian Y, Kurosawa T, Matsui S, Touma M, Wu Q, Sugimoto K: **Inhibition of blood vessel formation in tumors by IL-18-polarized M1 macrophages**. *Genes to cells : devoted to molecular & cellular mechanisms* 2016, **21**(3):287-295.

58. Sugimoto K, Yoshida S, Mashio Y, Toyota N, Xing Y, Xu H, Fujita Y, Huang Z, Touma M, Wu Q: **Role of FGF10 on tumorigenesis by MS-K**. *Genes to cells : devoted to molecular & cellular mechanisms* 2014, **19**(2):112-125.

59. Xu H, Toyota N, Xing Y, Fujita Y, Huang Z, Touma M, Wu Q, Sugimoto K: **Enhancement of phagocytosis and cytotoxicity in macrophages by tumor-derived IL-18 stimulation**. *BMB Reports* 2014, **47**(5):286-291.

60. Xing Y, Tian Y, Kurosawa T, Matsui S, Touma M, Yanai T, Wu Q, Sugimoto K: **CCL11-induced eosinophils inhibit the formation of blood vessels and cause tumor necrosis**. *Genes to cells : devoted to molecular & cellular mechanisms* 2016, **21**(6):624-638.

61. Lewis BP, Shih IH, Jones-Rhoades MW, Bartel DP, Burge CB: **Prediction of mammalian microRNA targets**. *Cell* 2003, **115**(7):787-798.

62. Chen HX, Cleck JN: **Adverse effects of anticancer agents that target the VEGF**

pathway. *Nature reviews Clinical oncology* 2009, **6**(8):465-477.

63. Zhong XY, Yoshioka A, Mashio Y, Ikeda T, Jiang H, Touma M, Wu Q, Wang C, Sugimoto K: **Effect of vegf gene knockdown on growth of the murine sarcoma cell line MS-K**. *Genes to cells : devoted to molecular & cellular mechanisms* 2011, **16**(6):625-638.

64. Kastan MB, Bartek J: **Cell-cycle checkpoints and cancer**. *Nature* 2004, **432**(7015):316-323.

65. Nojima H: **G1 and S-phase checkpoints, chromosome instability, and cancer**. *Methods in molecular biology* 2004, **280**:3-49.

66. Gartel AL, Serfas MS, Tyner AL: **p21--negative regulator of the cell cycle**. *Proceedings of the Society for Experimental Biology and Medicine Society for Experimental Biology and Medicine* 1996, **213**(2):138-149.

67. Sun F, Fu H, Liu Q, Tie Y, Zhu J, Xing R, Sun Z, Zheng X: **Downregulation of CCND1 and CDK6 by miR-34a induces cell cycle arrest**. *FEBS letters* 2008, **582**(10):1564-1568.

68. Evan GI, Vousden KH: **Proliferation, cell cycle and apoptosis in cancer**. *Nature* 2001, **411**(6835):342-348.

69. Bonecchi R, Galliera E, Borroni EM, Corsi MM, Locati M, Mantovani A: **Chemokines and chemokine receptors: an overview**. *Frontiers in bioscience* 2009, **14**:540-551.

70. Sun X, Cheng G, Hao M, Zheng J, Zhou X, Zhang J, Taichman RS, Pienta KJ, Wang J: **CXCL12 / CXCR4 / CXCR7 chemokine axis and cancer progression**. *Cancer metastasis reviews* 2010, **29**(4):709-722.

71. Ali S, Lazennec G: **Chemokines: novel targets for breast cancer metastasis**. *Cancer metastasis reviews* 2007, **26**(3-4):401-420.

72. Raman D, Baugher PJ, Thu YM, Richmond A: **Role of chemokines in tumor growth**. *Cancer letters* 2007, **256**(2):137-165.

73. Sanchez-Martin L, Estecha A, Samaniego R, Sanchez-Ramon S, Vega MA, Sanchez-Mateos P: **The chemokine CXCL12 regulates monocyte-macrophage differentiation and RUNX3 expression**. *Blood* 2011, **117**(1):88-97.

74. Osada H, Takahashi T: **MicroRNAs in biological processes and carcinogenesis**. *Carcinogenesis* 2007, **28**(1):2-12.

75. Fish JE, Srivastava D: **MicroRNAs: opening a new vein in angiogenesis research**. *Science signaling* 2009, **2**(52):pe1.

76. Tian Y, Matsui S, Touma M, Wu Q, Sugimoto K: **MicroRNA-342 inhibits tumor growth via targeting chemokine CXCL12 involved in macrophages recruitment/activation**. *Genes to cells : devoted to molecular & cellular mechanisms* 2018, **23**(12):1009-1022.

77. Dooley J, Lagou V, Pasciuto E, Linterman MA, Prosser HM, Himmelreich U, Liston A: **No Functional Role for microRNA-342 in a Mouse Model of Pancreatic Acinar Carcinoma**. *Frontiers in oncology* 2017, **7**:101.

78. Xie X, Liu H, Wang M, Ding F, Xiao H, Hu F, Hu R, Mei J: **miR-342-3p targets RAP2B to suppress proliferation and invasion of non-small cell lung cancer cells**. *Tumour biology : the journal of the International Society for Oncodevelopmental Biology and Medicine* 2015, **36**(7):5031-5038.

79. Leivonen SK, Sahlberg KK, Makela R, Due EU, Kallioniemi O, Borresen-Dale AL, Perala M: **High-throughput screens identify microRNAs essential for HER2 positive breast cancer cell growth**. *Molecular oncology* 2014, **8**(1):93-104.

80. Tai MC, Kajino T, Nakatochi M, Arima C, Shimada Y, Suzuki M, Miyoshi H, Yatabe Y, Yanagisawa K, Takahashi T: **miR-342-3p regulates MYC transcriptional activity via direct repression of E2F1 in human lung cancer**. *Carcinogenesis* 2015, **36**(12):1464-1473.

81. Hanahan D, Weinberg RA: **Hallmarks of cancer: the next generation**. *Cell* 2011, **144**(5):646-674.

82. Etzrodt M, Cortez-Retamozo V, Newton A, Zhao J, Ng A, Wildgruber M, Romero P, Wurdinger T, Xavier R, Geissmann F *et al*: **Regulation of monocyte functional heterogeneity by miR-146a and Relb**. *Cell reports* 2012, **1**(4):317-324.

83. Zhang Y, Zhang M, Zhong M, Suo Q, Lv K: **Expression profiles of miRNAs in polarized macrophages**. *International journal of molecular medicine* 2013, **31**(4):797-802.

84. Czimmerer Z, Varga T, Kiss M, Vazquez CO, Doan-Xuan QM, Ruckerl D, Tattikota SG, Yan X, Nagy ZS, Daniel B *et al*: **The IL-4/STAT6 signaling axis establishes a**

conserved microRNA signature in human and mouse macrophages regulating cell survival via miR-342-3p. *Genome medicine* 2016, **8**(1):63.

Supplemental Table 1. List of PCR primers.

Table S1 Primers used in this study.

Primer	**Sequence (5'-3', forward / reverse)**
miR-342	TCTCACACAGAAATCGCACCCGT
SnoRNA-202	TGAACCCTTTTCCATCT
Cxcl12	GCTCTGCATCAGTGACGGTA
	TAATTTCGGGTCAATGCACA
Vegf-A	TACCCTGGCTTTACTGCTGTA
	GTGAGGTTTGATCCGGATGAT
Vegf-C	AACGTGTCCAAGAAATCAGCC
	AGTCCTCTCCCGGAGTAATCC
ZsGreen1	CAAGTTCTACGGCGTGAACTTCC
	TCAGGTGCCACTTCTGGTTCT
Cxcr4	GTAGAGCGAGTGTTGCCATG
	TTGAAATGGACGTTTTCATCC
Cxcr7	AGCCTGGCAACTACTCTGACA
	TTGAAATGGACGTTTTCATCC
Thbs-1	AGTCGGGGCAGGAAGACTAT
	ACTGGGCTGGGTTGTAATGG
Cd80	CTGAAGACCGAATCTACTGGCAA
	CCTTTTAGTGTCTGCAGATGGGT
Cd86	AGGAACAACTGGACTCTACGACT
	TTCTTAGGTTTCGGGTGACCTTG
Cd163	ATGGGTGGACACAGAATGGTT
	CAGGAGCGTTAGTGACAGCAG
Dectin1	TGGGTTTAGGAATCCTGTGCTTTG
	CTGGGGAGCTGTATTTCTGACTTG
Ym1	TTGTGGGATTTCCAGCATATGGG

	ACGGCACCTCCTAAATTGTTGTC
Chi3l3	ACTTTGATGGCCTCAACCTG
	AATGATTCCTGCTCCTGTGG
Il-10	ACATACTGCTAACCGACTCCT
	ACTCTTCACCTGCTCCACT
Msr-1	TGATCGGGGACAAATTGGCT
	GTGCACAGCTAGAACTTCTTGG
Evl	ACGGAAGACCCTAGCACCTC
	CACAGACGGGGTTCTGGAC
β-actin	CAGGGTGTGATGGTGGGAATGGG
	CAGGATGGCGTGAGGGAGAGCA

Supplemental figure S1. Expression of *Cxcl12* and *Cxcr4* in tumor infiltrated CD11b-positive cells.

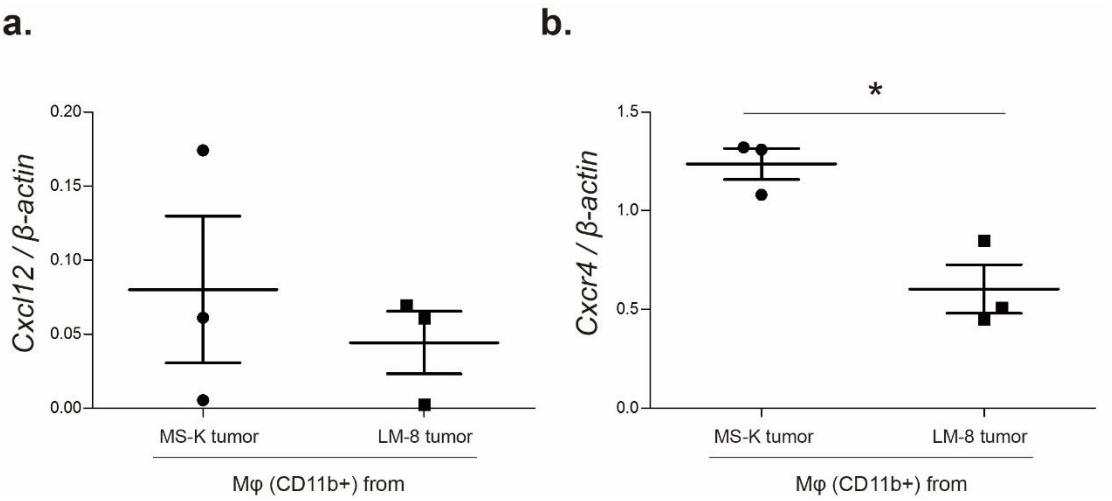

Acknowledgements

Many people have offered me valuable help in my doctoral program, including my supervisor, my colleagues, and my parents. I would like to express my gratitude to all those who have helped me.

First and foremost, I gratefully acknowledge the help of my supervisor Dr. Sugimoto. I do appreciate his patience, encouragement, and professional instructions during my doctoral program.

Meanwhile, I would like to extend my sincere gratitude to Dr. Touma, for her instructive advice and useful suggestions on my progress of the research. And also Professor Wu Qiong (Harbin University), who kindly gifted a luciferase vector.

I shall express my heartfelt gratitude to the members in Sugimoto Lab, Dr. Xu, Dr. Xing, Ms. Matsui, Mr. Kurosawa, and Ms. Kato, for their help in the lab.

I feel grateful to all my professors and teachers in Graduate School of Science and Technology who once offered me valuable courses and advice during my study.

Special thanks should go to my friends who have put considerable time and effort into their comments on the draft.

Last but not the least, my gratitude also extends to my beloved family who have been assisting, supporting and caring for me all of my life.